Available online at http://scik.org
Commun. Math. Biol. Neurosci. 2024, 2024:72
https://doi.org/10.28919/cmbn/8530
ISSN: 2052-2541

EFFECTS OF FEAR AND REFUGE STRATEGY DEPENDENT ON PREDATOR IN FOOD WEB DYNAMICS

HUSSEIN SABAH ABDULLAH, DAHLIA KHALED BAHLOOL*

Department of Mathematics, College of science, University of Baghdad, Baghdad, Iraq

Abstract: This study will address a prey and predator model, incorporating a fear coefficient within the prey population. The predator category comprises two distinct types: active predators and scavengers. An assessment will be conducted to examine the influence of refuges on the predator dynamics and the broader system dynamics within the food web. Due to the importance of scavengers for environmental sustainability in waste management, this research was interested in studying the dynamic behavior of the ecosystem consisting of prey-predator-scavengers. Fear of predation, refugees, and harvesting are the biological factors included in the mathematical model to understand their influence on the dynamic behavior of the proposed model. The study comprises a thorough examination of the limitations of solutions, followed by the calculation of equilibrium points. The local and global stability of all points of equilibrium are studied. All the sufficient conditions for the occurrence of local bifurcation are identified. The conditions for the persistence of the model are created. Finally, the numerical solution is utilized to validate our theoretical results and understand the effect of changing parameter values on dynamic behavior. All numerical results were calculated using the Mathematica program. Visual aids, such as diagrams, were employed to enhance clarity in depicting their effects on both predators and the overarching system.

Keywords: prey-predator model; cooperation; refuge; fear; scavenger; bifurction; ecology; food web.

2020 AMS Subject Classification: 34D20, 92D40,34C23.

---

*Corresponding author
E-mail address: dahlia.khaled@sc.uobaghdad.edu.iq
Received March 08, 2024

1. INTRODUCTION

Due to its generality and importance, the interaction between predators and their prey has long been and is going on to be one of the major threats in ecology and its mathematical formulation [1]. A prey-predator model is a mathematical depiction that explains the dynamics between the predator and prey populations that interact within an ecosystem. These models are usually composed of a system of differential equations that characterize the time-dependent changes in populations as a result of their interactions. The Lotka-Volterra model, which describes the link between a predator and prey, is the framework of the system. Because of their intricate dynamics and significant effects on ecosystems, prey-predator interactions have long piqued the interest of ecologists and biologists. In mathematical biology, several dynamical behavior models among predators and their prey have been checked [2-9]. Many studies to understand the dynamics of trigeneric food chains have been completed [10-15]. Most of them focused on the presence and extinction of living organisms in them [16-20]. On the other hand, previous studies have dealt with understanding the dynamics of trigeneric diets [21-25].

The idea of predator dependency emerges from these interactions as a key factor influencing how ecological groups balance out. The degree to which a prey species relies on predation pressure to control its population dynamics, habitat distribution, and behavioral characteristics is known as predator dependency [26]. Predator dependency is important, but it goes much beyond simple survival tactics; it includes intricate evolutionary adaptations and feedback loops in ecosystems. Predators adapt in response to prey species' evolution of defense systems so they can preserve their food supply. Co-evolution is a complex dance that frequently produces ecological systems that are highly tuned and in which even little disturbances may have far-reaching effects. Predator dependency comes in various forms in reality. The fear generated by the predation process is inherently dependent on the ferocity and number of predators, which leads the prey to adapt its diet and reproduction as a result of hiding out of fear. In addition, the shelters in which the prey refuges from predation depend on the predators and their danger [27-28]. Many researchers have recently taken up the study of the dynamics of the prey-predator model when fear is present [29-

37]. Those studies have expanded to include the effect of fear on the dynamic behavior of both food chains and food webs [39-42]. However, Ahmed and Bahlool [38] proposed and studied a mathematical model of a Holling type-II food web comprising prey-predator-scavenger in the case of the existence of fear and quadratic harvesting. They obtained that the solution appears to approach either the asymptotic stable point or a Hopf-bifurcation. Furthermore, both fear and harvesting have a stabilizing effect on the system's behavior up to a certain point, and then extinction occurs.

Research has expanded to explore the effect of the fear factor on the dynamic behavior of food chains and food webs. Some researchers also studied the effect of the presence of a refuge in the prey on the dynamic behavior of predatory prey models, as we see in [43-45]. After that, studies were prepared that directed researchers to study the effect of the factors of fear and refuge on behavior. The system is as in [46]. In addition to the above, due to the importance of scavengers, they contribute to the sustainability of the environment through waste management and the identification and classification of organic and inorganic waste. Therefore, some researchers have recently taken up the study of ecosystems in the presence of scavengers to understand the dynamic behavior of food chains and preserve the environment through the preservation of these organisms. Satar and Naji [47–48] proposed and studied mathematical models that describe the interaction between prey-predator-scavenger in cases of the existence and non-existence of toxicants. In contrast to the above, this paper combines fear, refuge, harvesting, and scavengers in a single food web model to bring it closer to reality than the models addressed by the above-mentioned studies. This paper is concerned with proposing and studying the dynamic behavior of the prey-predator-scavenger food web and the extent of the impact of fear and shelter dependent on the predator in it.

2. MODEL DESCRIPTION

The prey-predator-scavenger model of a three-species ecological system is examined in this work. According to the model, a linear form of the Holling Type-I functional response is used by the first species (prey) to be consumed by the second species (predator) and the third species (scavenger). When their only source of food is gone, the number of predators decreases dramatically. The carcasses of predators are another source of food for scavengers. Without food, they decay at an exponential rate. Because of the fear impact, the predation process reduces the prey's growth. Due to this, the prey uses the refuge, which is dependent on the number of predators, to protect themselves. Lastly, a quadratic harvesting process affects the predator and scavenger. These hypotheses allow the following set of nonlinear ordinary differential equations to accurately describe the population dynamics of this ecological model:

$$\begin{aligned} \frac{dX}{dT} &= \frac{rX}{1+f(Y+Z)} - bX^2 - a_1(1-cY)XY - a_2(1-cZ)XZ, \\ \frac{dY}{dT} &= e_1a_1(1-cY)XY - d_1Y - q_1E_1Y^2, \\ \frac{dZ}{dT} &= e_2a_2(1-cZ)XZ + a_3YZ - d_2Z - q_2E_2Z^2. \end{aligned} \tag{1}$$

The populations of prey, predator, and scavenger are denoted as $X(T), Y(T)\ and\ Z(T)$ respectively in the given equation. All the parameters in the system (1) are required to be non-negative.

Table 1. Biological significance of each parameter.

Parameter	Description
r	Growth rate of the prey.
f	The fear levels.
b	The intraspecific competition of prey species
a_1 , a_2	Attack rates of predator and scavenger, respectively.
a_3	The conversion rate of the predator's carcass biomass to scavenger.
$(1-cY)$, $(1-cZ)$	Predator-dependent refuge rates, where c denotes the coefficient of prey refuge in (0, 1) with $Y < \frac{1}{c}$ and $Z < \frac{1}{c}$, respectively.
e_1 , e_2	The conversion rates of prey biomass to predator and scavenger, respectively, which belong to (0, 1).
d_1 , d_2	The mortality rates of predator and scavenger, respectively.
q_1 , q_2	The catchability constant of predator and scavenger, respectively.
E_1 , E_2	The harvesting efforts of predator and scavenger, respectively.

3. Dimensionless Form of the Model

The transformation of a model into a dimensionless form involves expressing the system using dimensionless quantities. This approach offers several advantages. Firstly, it minimizes the number of parameters, simplifying the analysis process. Secondly, it enables better comparison of parameters in terms of their magnitudes, allowing for deeper insights into the system. Additionally, it facilitates comparisons between different systems. Thus, the equation (1) can be reformulated as follows:

$$\begin{aligned} \frac{dx}{dt} &= xf_1(x,y,z), \\ \frac{dy}{dt} &= yf_2(x,y,z), \\ \frac{dz}{dt} &= zf_3(x,y,z). \end{aligned} \tag{2}$$

where

$$f_1(x,y,z) = \frac{1}{1+w_0(y+z)} - x - w_1(1-y)y - w_2(1-z)z,$$

$$f_2(x,y,z) = w_3(1-y)x - w_4 - w_5 y,$$

$$f_3(x,y,z) = w_6(1-z)x + w_7 y - w_8 - w_9 z.$$

with the dimensionless variables and parameters given by:

$$t = rT\ ,\ x = \frac{b}{r}X\ ,\ y = cY\ ,\ z = cZ,$$

$$w_0 = \frac{f}{c}\ , w_1 = \frac{a_1}{rc}\ , w_2 = \frac{a_2}{rc}\ , w_3 = \frac{e_1 a_1}{b}\ ,\ w_4 = \frac{d_1}{r}\ ,$$

$$w_5 = \frac{q_1 E_1}{rc}, w_6 = \frac{e_2 a_2}{b}\ , w_7 = \frac{a_3}{rc}\ , w_8 = \frac{d_2}{r}\ , w_9 = \frac{q_2 E_2}{rc}\ .$$

Theorem 1. The solutions of the system (2) are uniformly bounded for all the initial conditions $x(0), y(0), z(0) > 0$.

Proof. From the first equation of system (2)

$$\frac{dx}{dt} = x\left[\frac{1}{1+w_0(y+z)} - x - w_1(1-y)y - w_2(1-z)z\right],$$

$$\frac{dx}{dt} \le x\left[\frac{1}{1+w_0(y+z)} - x\right] \le x(1-x).$$

Then solving the above differential inequality gives that $x(t) \le 1$ as $t \to \infty$.

Now, define the function: $H_1(t) = x(t) + \frac{w_1}{w_3}y(t)$.

After performing some algebraic calculations, we obtain the following result:

$$\frac{dH_1}{dt} \leq x - \frac{w_1 w_4}{w_3} y \leq x(1 + w_4) - w_4 \left(x + \frac{w_1}{w_3} y\right).$$

Then by using the bound of x, it is obtained that:

$$\frac{dH_1}{dt} + w_4 H_1 \leq (1 + w_4).$$

By solving this differential inequality, we obtain that $H_1 \leq \frac{(1+w_4)}{w_4}$,

for $t \to \infty$, and this leads to $y \leq \frac{w_3(1+w_4)}{w_1 w_4} = \beta_1$,

Now, we define $H_2(t) = x(t) + \frac{w_1}{w_3} y(t) + \frac{w_2}{w_6} z(t)$, then

$$\frac{dH_2}{dt} \leq 2x - x - \frac{w_1 w_4}{w_3} y - \left[\frac{w_2 w_8 - w_2 w_7 \beta_1}{w_6}\right] z,$$

$$\leq 2 - \mu \left[x + \frac{w_1}{w_3} y + \frac{w_2}{w_6} z\right].$$

where $\mu = \min\{1, w_4, w_8 - w_7 \beta_1\}$. This implies that:

$$\frac{dH_2}{dt} + \mu H_2 \leq 2$$

Again, solving the last differential inequality, gives $H_2 \leq \frac{2}{\mu}$, for $t \to \infty$.

Hence, our system is uniformly bounded and that guarantees their validity.

4. THE EQUILIBRIUM POINTS

By setting all the equations in the system (2) equal to zero and solving for the variables $x(t), y(t), and\ z(t)$, we can determine the equilibrium points.

$$\begin{aligned} x f_1(x, y, z) &= 0 \\ y f_2(x, y, z) &= 0 \\ z f_3(x, y, z) &= 0 \end{aligned} \tag{3}$$

Consequently, the following solutions (equilibrium points) are obtained:

The evanescence equilibrium point, $Q_0 = (0,0,0)$, always exists.

The axial equilibrium point, $Q_1 = (1,0,0)$, always exists.

The scavenger-free equilibrium point, $Q_{xy} = (\hat{x}, \hat{y}, 0)$, where:

$$\hat{x} = \frac{w_4 + w_5 \hat{y}}{w_3(1 - \hat{y})} \tag{4}$$

while $\hat{y}$ is a positive root of the $4th$ order equation.

$$\varsigma_1 y^4 + \varsigma_2 y^3 + \varsigma_3 y^2 + \varsigma_4 y + \varsigma_5 = 0,$$

where:

$$\varsigma_1 = -w_0 w_1 w_3,$$

$$\varsigma_2 = 2w_0 w_1 w_3 - w_1 w_3,$$

$$\varsigma_3 = 2w_1 w_3 - w_0 w_1 w_3 - w_0 w_5,$$

$$\varsigma_4 = -w_3 - w_5 - w_0 w_4 - w_1 w_3,$$

$$\varsigma_5 = w_3 - w_4.$$

Direct computation shows that the positive root exists uniquely, and hence there is a unique point, say Q_{xy} within the interior of the first quadrant of the $xy - plane$, if the following sufficient conditions are satisfied

$$1 > \hat{y}, \tag{5a}$$

$$w_3 > w_4, \tag{5b}$$

$$\frac{2w_1 w_3}{w_1 w_3 + w_5} < w_0 < \frac{1}{2}. \tag{5c}$$

The predator-free equilibrium point, $Q_{xz} = (\bar{x}, 0, \bar{z})$, where

$$\bar{x} = \frac{w_8 + w_9 \bar{z}}{w_6(1-\bar{z})}. \tag{6}$$

while $\bar{z}$ is a positive root of the $4th$ order equation.

$$\alpha_1 z^4 + \alpha_2 z^3 + \alpha_3 z^2 + \alpha_4 z + \alpha_5 = 0.$$

where

$$\alpha_1 = -w_0 w_2 w_6,$$

$$\alpha_2 = 2w_0 w_2 w_6 - w_2 w_6,$$

$$\alpha_3 = 2w_2 w_6 - w_0 w_2 w_6 - w_0 w_9,$$

$$\alpha_4 = -w_6 - w_9 - w_0 w_8 - w_2 w_6,$$

$$\alpha_5 = w_6 - w_8.$$

Direct computation shows that the positive root exists uniquely, and hence there is a unique point, namely Q_{xz} within the interior of the first quadrant of the $xz - plane$, if the following sufficient conditions are satisfied:

$$1 > \bar{z}, \tag{7a}$$

$$w_6 > w_8, \tag{7b}$$

$$\frac{2w_2w_6}{w_2w_6+w_9} < w_0 < \frac{1}{2}. \tag{7c}$$

The coexistence (positive) equilibrium point, $Q_{xyz} = (x^*, y^*, z^*)$, where

$$\begin{aligned} x^* &= \frac{w_4+w_5y^*}{w_3(1-y^*)}, \\ z^* &= \frac{w_3(w_7y^*-w_8)(y^*-1)-w_5w_6y^*-w_4w_6}{w_3w_9(y^*-1)-w_6(w_5y^*+w_4)}. \end{aligned} \tag{8a}$$

while y^* is a positive root of the $7th$ order equation:

$$\mu_1y^7 + \mu_2y^6 + \mu_3y^5 + \mu_4y^4 + \mu_5y^3 + \mu_6y^2 + \mu_7y + \mu_8 = 0. \tag{8b}$$

where the coefficients $\mu_i, i = 1,2,\dots,8$ are determined using Mathematica program, and because of their huge and complicated forms it will not be given here. Direct computation shows that the positive equilibrium point Q_{xyz} exists uniquely, in the interior of first octant, if there is a unique positive root for the equation (8b) that satisfies the following conditions:

$$y^* < 1, \tag{9a}$$

$$w_3(w_7y^* - w_8)(y^* - 1) - w_5w_6y^* - w_4w_6 < 0, \tag{9b}$$

$$\left.\begin{matrix} \mu_1 < 0, \mu_8 > 0 \\ or \\ \mu_1 > 0, \mu_8 < 0 \end{matrix}\right\}. \tag{9c}$$

5. LOCAL STABILITY ANALYSIS

We examine the local stability of every equilibrium point by utilizing the Jacobian matrix and determining the eigenvalues near each point. The Jacobian matrix H for three-dimensional systems can be determined by:

$$H(x,y,z) = \begin{bmatrix} f_1 + x\frac{\partial f_1}{\partial x} & x\frac{\partial f_1}{\partial y} & x\frac{\partial f_1}{\partial z} \\ y\frac{\partial f_2}{\partial x} & f_2 + y\frac{\partial f_2}{\partial y} & y\frac{\partial f_2}{\partial z} \\ z\frac{\partial f_3}{\partial x} & z\frac{\partial f_3}{\partial y} & f_3 + z\frac{\partial f_3}{\partial z} \end{bmatrix}. \tag{10}$$

where

$$\frac{\partial f_1}{\partial x} = -1, \ \frac{\partial f_1}{\partial y} = -w_1(1-y) + w_1y - \frac{w_0}{(1+w_0(y+z))^2},$$

$$\frac{\partial f_1}{\partial z} = -\mathrm{w}_2(1-z) + \mathrm{w}_2 z - \frac{\mathrm{w}_0}{(1+\mathrm{w}_0(y+z))^2},$$

$$\frac{\partial f_2}{\partial x} = w_3 - w_3 y,\ \frac{\partial f_2}{\partial y} = -\mathrm{w}_5 - \mathrm{w}_3 x,\ \frac{\partial f_2}{\partial z} = 0,$$

$$\frac{\partial f_3}{\partial x} = \mathrm{w}_6(1-z),\ \frac{\partial f_3}{\partial y} = \mathrm{w}_7,\ \frac{\partial f_3}{\partial z} = -\mathrm{w}_9 - \mathrm{w}_6 x.$$

By replacing the equilibrium points mentioned above individually in the Jacobian matrix $H(x, y, z)$ and subsequently calculating their eigenvalues, it can be noted that:

The eigenvalues of the Jacobian matrix (10) at the evanescence equilibrium point (Q_0) are (1, $-w_4$, $-w_8$), which indicates that Q_0 represents a saddle point.

The eigenvalues of the Jacobian matrix (10) at the axial equilibrium point (Q_1) are computed as:

$$\lambda_{11} = -1, \lambda_{12} = w_3 - w_4,\ \lambda_{13} = w_6 - w_8. \tag{11}$$

Therefore, Q_1 exhibits local asymptotic stability if and only if the following conditions are satisfied:

$$w_3 < w_4. \tag{12a}$$

$$w_6 < w_8. \tag{12b}$$

The Jacobian matrix can be expressed in terms of the equilibrium point where scavengers are absent:

$$H(Q_{xy}) = \begin{bmatrix} -\hat{x} & \hat{x}\left(2w_1\hat{y} - w_1 - \frac{w_0}{(1+w_0\hat{y})^2}\right) & \hat{x}\left(-w_2 - \frac{w_0}{(1+w_0\hat{y})^2}\right) \\ \hat{y}(w_3 - w_3\hat{y}) & -\mathrm{w}_5\hat{y} - \mathrm{w}_3\hat{x}\hat{y} & 0 \\ 0 & 0 & w_6\hat{x} + w_7\hat{y} - w_8 \end{bmatrix}. \tag{13}$$

The equation that describes the characteristics equation of $H(Q_{xy})$ can be represented in the following form:

$$(\lambda^2 - T_{xy}\lambda + D_{xy})(w_6\hat{x} + w_7\hat{y} - w_8 - \lambda) = 0. \tag{14}$$

where:

$$T_{xy} = -w_5\hat{y} - w_3\hat{x}\hat{y} - \hat{x},$$

$$D_{xy} = -w_3\hat{x}\hat{y}(1-\hat{y})\left(2w_1\hat{y} - w_1 - \frac{w_0}{(1+w_0\hat{y})^2}\right) + \hat{x}\hat{y}(w_5 + w_3\hat{x}).$$

Consequently, the eigenvalues of the matrix $H(Q_{xy})$ are identified as $\lambda_{2i} = \frac{T_{xy}}{2} \pm$

$\frac{1}{2}\sqrt{T_{xy}{}^{2}-4D_{xy}}$, for $i=1,2$ and $\lambda_{23}=w_6\hat{x}+w_7\hat{y}-w_8$. Hence, if the following conditions are met, all eigenvalues will possess negative real parts, indicating that Q_{xy} is locally asymptotically stable.

$$w_6\hat{x}+w_7\hat{y}<w_8, \tag{15a}$$

$$\hat{y}<\frac{1}{2}+\frac{w_0}{2w_1(1+w_0\hat{y})^2}. \tag{15b}$$

The Jacobian matrix can be expressed as follows when considering the equilibrium point without predators:

$$H(Q_{xz})=\begin{bmatrix} -\bar{x} & -\bar{x}\left(w_1+\frac{w_0}{(1+w_0\bar{z})^2}\right) & \bar{x}\left(2w_2\bar{z}-w_2-\frac{w_0}{(1+w_0\bar{z})^2}\right) \\ 0 & -\mathrm{w}_4+\mathrm{w}_3\bar{x} & 0 \\ w_6\bar{z}-w_6\bar{z}^2 & w_7\bar{z} & -w_9\bar{z}-w_6\bar{x}\bar{z} \end{bmatrix}. \tag{16}$$

The expression for the characteristic equation of $H(Q_{xz})$ can be formulated in the following manner.

$$[\lambda^2-T_{xz}\lambda+D_{xz}][-w_4+w_3\bar{x}]=0, \tag{17}$$

where:

$$T_{xz}=-\bar{x}-w_9\bar{z}-w_6\bar{x}\bar{z},$$

$$D_{xz}=-w_6\bar{x}\bar{z}(1-\bar{z})\left(2w_2\bar{z}-w_2-\frac{w_0}{(1+w_0\bar{z})^2}\right)+\bar{x}\bar{z}(w_9+w_6\bar{x}).$$

Consequently, the eigenvalues of the matrix $H(Q_{xz})$ are identified as $\lambda_{3i}=\frac{T_{xz}}{2}\pm\frac{1}{2}\sqrt{T_{xz}{}^{2}-4D_{xz}}$, for $i=1,3$ and $\lambda_{32}=-\mathrm{w}_4+\mathrm{w}_3\bar{x}$. Hence, if the following conditions are met, all eigenvalues will possess negative real parts, indicating that Q_{xz} is locally asymptotically stable.

$$\bar{x}<\frac{w_4}{w_3}, \tag{18a}$$

$$\bar{z}<\frac{1}{2}+\frac{w_0}{2w_2(1+w_0\bar{z})^2}. \tag{18b}$$

Theorem 2. The coexistence equilibrium point of system (2) will be locally asymptotically stable if the conditions listed below are satisfied.

$$2w_1y^*<w_1+\frac{w_0}{\left(1+w_0(y^*+z^*)\right)^2}, \tag{19a}$$

$$2w_2z^* < w_2 + \frac{w_0}{\left(1+w_0(y^*+z^*)\right)^2}, \tag{19b}$$

$$y^* < 1, \tag{19c}$$

$$z^* < 1, \tag{19d}$$

$$a_{11}a_{22}a_{33} - a_{13}a_{21}a_{32} < 0. \tag{19e}$$

where a_{ij} for all $i,j = 1,2,3$ represent the Jacobian matrix elements at Q_{xyz} and it will be given in the proof.

Proof. The Jacobian matrix of the system (2) at $Q_{xyz} = (x^*, y^*, z^*)$, can be written as:

$$H(Q_{xyz}) = [a_{ij}]_{3\times 3}. \tag{20}$$

where:

$$a_{11} = -x^*,\ a_{12} = x^*\left(2w_1y^* - w_1 - \frac{w_0}{\left(1+w_0(y^*+z^*)\right)^2}\right),$$

$$a_{13} = x^*\left(2w_2z^* - w_2 - \frac{w_0}{\left(1+w_0(y^*+z^*)\right)^2}\right),$$

$$a_{21} = w_3y^* - w_3y^{*2}, \quad a_{22} = -w_5y^* - w_3x^*y^*, \quad a_{23} = 0,$$

$$a_{31} = w_6z^* - w_6z^{*2}, \quad a_{32} = w_7z^*, \quad a_{33} = -w_9z^* - w_6x^*z^*.$$

Hence, the characteristic equation of $H(Q_{xyz})$ can be expressed as:

$$\lambda^3 + A\lambda^2 + B\lambda + C = 0. \tag{21}$$

where

$$A = -(a_{11} + a_{22} + a_{33}),$$

$$B = a_{11}a_{22} - a_{12}a_{21} + a_{11}a_{33} - a_{13}a_{31} + a_{22}a_{33},$$

$$C = -(a_{11}a_{22}a_{33} + a_{13}a_{21}a_{32} - a_{13}a_{22}a_{31} - a_{12}a_{21}a_{33}).$$

With

$$\Delta = AB - C = -(a_{11}+a_{22})(a_{11}a_{22} - a_{12}a_{21}) - a_{11}a_{22}a_{33} + a_{13}a_{21}a_{32}$$
$$-(a_{11}+a_{33})(a_{11}a_{33} - a_{13}a_{31}) - (a_{22}a_{33})(a_{11}+a_{22}+a_{33}).$$

It should be noted that applying the Routh-Hurwitz criterion requires satisfying the conditions $A > 0$, $C > 0$, and $\Delta > 0$, which guarantees that all the roots of equation (21) have negative real parts. By performing direct calculations, it can be shown that the conditions (19a), (19b), (19c), (19d) and (19e) are sufficient to fulfill all the requirements of the Routh-Hurwitz criterion. Consequently, Q_{xyz} achieves local asymptotic stability. □

6. GLOBAL STABILITY

In this section, the method of the Lyapunov function is employed to determine the basin of attraction associated with each locally asymptotically stable point in the domain $\mathbb{R}_+^3$. If the basin of attraction for an equilibrium point encompasses the whole domain $\mathbb{R}_+^3$, it is considered globally asymptotically stable. As given in the following theorems.

Theorem 3. The local asymptotic stability of Q_1 implies its global asymptotic stability if the conditions outlined below are satisfied.

$$\frac{w_1 w_4}{w_3} > w_0 + w_1. \tag{22a}$$

$$\frac{w_2 w_8}{w_6} > (w_0 + w_2) + \frac{w_2 w_7}{w_6}\beta_1, \tag{22b}$$

Proof. The real-valued function $\mathrm{W}_1 = \mathrm{k}_1 \int_{\breve{x}}^{x} \frac{u-\breve{x}}{u} du + \mathrm{k}_2 y + \mathrm{k}_3 z$, is defined with $\breve{x} = 1$. By performing direct calculations, it can be shown that $\mathrm{W}_1: M_1 \to \mathbb{R}$, when $M_1 = \{(x, y, z) \in \mathbb{R}_+^3 : x > 0, y \geq 0, z \geq 0\}$.

Consequently, this implies $\mathrm{W}_1(Q_1) = 0$, and $\mathrm{W}_1(x, y, z) > 0$, for every $(x, y, z) \in M_1 - Q_1$. Furthermore, simple calculations yield that:

$$\frac{d\mathrm{W}_1}{dt} = \mathrm{k}_1 \frac{dx}{dt}\left(\frac{x-\breve{x}}{x}\right) + \mathrm{k}_2 \frac{dy}{dt} + \mathrm{k}_3 \frac{dz}{dt},$$

$$\frac{d\mathrm{W}_1}{dt} \leq -k_1(x-\breve{x})^2 + k_1 \frac{w_0\,\breve{x}y}{1+w_0(y+z)} + k_1 \frac{w_0 \breve{x} z}{1+w_0(y+z)}$$
$$-(k_1 w_1 - k_2 w_3)(1-y)xy - (k_1 w_2 - k_3 w_6)(1-z)xz$$
$$+k_1 w_1 \breve{x} y + k_1 w_2 \breve{x} z - k_2 w_4 y + k_3 w_7 yz - k_3 w_8 z.$$

By choosing positive constant values as $\mathrm{k}_1 = 1, \mathrm{k}_2 = \frac{\mathrm{w}_1}{w_3}$, and $\mathrm{k}_3 = \frac{\mathrm{w}_2}{w_6}$, and applying the concept of maximization with an upper bound constant β_1, the following results are obtained:

$$\frac{d\mathrm{W}_1}{dt} \leq -\left(\frac{w_1 w_4}{w_3} - w_0 - w_1\right) y - \left(\frac{w_2 w_8}{w_6} - \frac{w_2 w_7}{w_6}\beta_1 - (w_0 + w_2)\right) z - (x-1)^2.$$

Therefore, conditions (22a) and (22b) imply that $\frac{d\mathrm{W}_1}{dt} < 0$. As a result, Q_1 exhibits global asymptotic stability. □

Theorem 4. The local asymptotic stability of Q_{xy} implies its global asymptotic stability if the conditions outlined below are satisfied.

$$\left[\frac{w_0}{[1+w_0(y+z)](1+w_0\hat{y})} - \mathrm{w}_1\hat{y}\right]^2 < 4\frac{w_1}{w_3}(w_3\hat{x} + w_5), \tag{23a}$$

$$\frac{w_0\hat{x}}{(1+w_0\hat{y})} + \mathrm{w}_2\hat{x} + \mathrm{w}_2 + \frac{w_2 w_7}{w_6}\beta_1 < \frac{w_2 w_8}{w_6}. \tag{23b}$$

Proof. The real-valued function $\mathrm{W}_2 = m\int_{\hat{x}}^{x}\frac{u-\hat{x}}{u}du + \mathrm{m}_2\int_{\hat{y}}^{y}\frac{v-\hat{y}}{v}dv + \mathrm{m}_3 z$, is defined. By performing direct calculations, it can be shown that $\mathrm{W}_2\colon M_2 \to \mathbb{R}$, when $M_2 = \{(x,y,z) \in \mathbb{R}_+^3 : x > 0, y > 0, z \geq 0\}$. Consequently, this implies $\mathrm{W}_2(Q_{xy}) = 0$, and $\mathrm{W}_2(x,y,z) > 0$ for every $(x,y,z) \in M_2 - Q_{xy}$. Furthermore, simple calculations yield that:

$$\frac{d\mathrm{W}_2}{dt} = \mathrm{m}_1\left(\frac{x-\hat{x}}{x}\right)\frac{dx}{dt} + \mathrm{m}_2\left(\frac{y-\hat{y}}{y}\right)\frac{dy}{dt} + \mathrm{m}_3\frac{dz}{dt}.$$

By employing direct computation incorporating the principle of maximizing, and using the upper bound constant of the variables x and y leads to the following outcome:

$$\begin{aligned}\frac{dW_2}{dt} \leq & -m_1(x-\hat{x})^2 - m_2(w_3\hat{x}+w_5)(y-\hat{y})^2 - (m_3w_6 - m_1w_2)\,xz^2 \\ & -\left(\frac{m_1w_0}{[1+w_0(y+z)](1+w_0\hat{y})} + m_1w_1 - m_1w_1\hat{y} - m_2w_3\right)(x-\hat{x})(y-\hat{y}) \\ & -(m_2w_3 - m_1w_1)(x-\hat{x})(y-\hat{y})y \\ & -\left(m_3w_8 - \frac{m_1w_0\hat{x}}{(1+w_0\hat{y})} - m_1w_2\hat{x} - m_3w_6 - m_3w_7\beta_1\right)z.\end{aligned}$$

Now, by choosing positive constant values as $m = 1, \mathrm{m}_2 = \frac{w_1}{w_3}$, and $\mathrm{m}_3 = \frac{\mathrm{w}_2}{w_6}$, the following results are obtained

$$\begin{aligned}\frac{dW_2}{dt} \leq & -(x-\hat{x})^2 - \frac{w_1}{w_3}(w_3\hat{x}+w_5)(y-\hat{y})^2 \\ & -\left(\frac{w_0}{[1+w_0(y+z)](1+w_0\hat{y})} - w_1\hat{y}\right)(x-\hat{x})(y-\hat{y}) \\ & -\left(\frac{w_2w_8}{w_6} - \frac{w_0\hat{x}}{(1+w_0\hat{y})} - w_2\hat{x} - w_2 - \frac{w_2w_7}{w_6}\beta_1\right)z.\end{aligned}$$

Using the conditions (23a) and (23b) it is obtained that:

$$\frac{dW_2}{dt} \le -\left[(x-\hat{x}) + \sqrt{\frac{w_1}{w_3}(w_3\hat{x}+w_5)}(y-\hat{y})\right]^2$$
$$-\left(\frac{w_2 w_8}{w_6} - \frac{w_0\hat{x}}{(1+w_0\hat{y})} - w_2\hat{x} - w_2 - \frac{w_2 w_7}{w_6}\beta_1\right) z.$$

Note that, $\frac{dW_2}{dt}$ is a negative definite function, and hence the proof is complete. □

Theorem 5. If the conditions outlined below are satisfied, the local asymptotic stability of Q_{xz} implies its global asymptotic stability.

$$\left[\frac{w_0}{(1+w_0\bar{z})} - \mathrm{w}_2\bar{z}\right]^2 < 4\frac{w_2}{w_6}(w_6\bar{x}+w_9), \tag{24a}$$

$$\frac{w_0\bar{x}}{(1+w_0\bar{z})} + \mathrm{w}_1\bar{x} + \mathrm{w}_1 + \frac{2w_7}{\mu} < \frac{w_1 w_4}{w_3} + \frac{w_2 w_7}{w_6}\bar{z}. \tag{24b}$$

where $\frac{2}{\mu}$ is the upper bound that is given in the theorem 1.

Proof. The real-valued function $\mathrm{W}_3 = \mathrm{p}_1\int_{\bar{x}}^{x}\frac{u-\bar{x}}{u}du + \mathrm{p}_2 y + \mathrm{p}_3\int_{\bar{z}}^{z}\frac{c-\bar{z}}{c}dc$, is defined. By performing direct calculations, it can be shown that $\mathrm{W}_3: M_3 \to \mathbb{R}$, when $M_3 = \{(x,y,z) \in \mathbb{R}_+^3 : x > 0, y \ge 0, z > 0\}$.

Consequently, this implies $\mathrm{W}_3(Q_{xz}) = 0$, and $\mathrm{W}_3(x,y,z) > 0$, for every $(x,y,z) \in M_3 - Q_{xz}$.

Furthermore, simple calculations yield that:

$$\frac{d\mathrm{W}_3}{dt} = \mathrm{p}_1\left(\frac{x-\bar{x}}{x}\right)\frac{dx}{dt} + \mathrm{p}_2\frac{dy}{dt} + \mathrm{p}_3\left(\frac{z-\bar{z}}{z}\right)\frac{dz}{dt}.$$

Likewise, employing the concept of maximizing allows for a direct calculation that results in:

$$\frac{dW_3}{dt} \le -p_1(x-\bar{x})^2 - p_3(w_6\bar{x}+w_9)(z-\bar{z})^2 - [p_2 w_3 - p_1 w_1]\, xy^2$$
$$-\left(\frac{p_1 w_0}{(1+w_0(y+z)(1+w_0\bar{z})} + p_1 w_2 - p_1 w_2\bar{z} - p_3 w_6\right)(x-\bar{x})(z-\bar{z})$$
$$-(p_3 w_6 - p_1 w_2) z(x-\bar{x})(z-\bar{z})$$
$$-\left[p_2 w_4 + p_3 w_7\bar{z} - \frac{P_1 w_0\bar{x}}{[1+w_0(y+z)](1+w_0\bar{z})} - p_1 w_1\bar{x} - p_2 w_3 - p_3 w_7 z\right] y.$$

By choosing positive constant values as $p_1 = 1, \mathrm{p}_2 = \frac{w_1}{w_3}$, and $\mathrm{p}_3 = \frac{\mathrm{w}_2}{w_6}$, the following results are obtained:

$$\frac{dW_3}{dt} \le -(x-\bar{x})^2 - \frac{\mathrm{w}_2}{w_6}(w_6\bar{x}+w_9)(z-\bar{z})^2$$

$$-\left(\frac{w_0}{(1+w_0(y+z)(1+w_0\bar{z})}-w_2\bar{z}\right)(x-\bar{x})(z-\bar{z})$$
$$-\left[\frac{w_1w_4}{w_3}+\frac{w_2w_7\bar{z}}{w_6}-\frac{P_1w_0\bar{x}}{(1+w_0\bar{z})}-w_1(\bar{x}+1)-\frac{2w_7}{\mu}\right]y.$$

Applying the given conditions (24a) - (24b) leads to the conclusion that:

$$\frac{dW_3}{dt}\leq-\left[(x-\bar{x})+\sqrt{\frac{w_2}{w_6}(w_6\bar{x}+w_9)}(z-\bar{z})\right]^2$$
$$-\left[\frac{w_1w_4}{w_3}+\frac{w_2w_7\bar{z}}{w_6}-\frac{P_1w_0\bar{x}}{(1+w_0\bar{z})}-w_1(\bar{x}+1)-\frac{2w_7}{\mu}\right]y.$$

Therefore, conditions (24a) and (24b) imply that $\frac{dW_3}{dt}<0$. As a result, Q_{xz} exhibits global asymptotic stability. □

Theorem 6. If the conditions outlined below are satisfied, the local asymptotic stability of Q_{xyz} implies its global asymptotic stability.

$$\left[\frac{w_0}{[1+w_0(y^*+z^*)]}-w_1y^*\right]^2<\frac{w_1}{w_3}(w_3x^*+w_5) \tag{25a}$$

$$\left[\frac{w_0}{[1+w_0(y^*+z^*)]}-w_2z^*\right]^2<\frac{w_2}{w_6}(w_6x^*+w_9) \tag{25b}$$

$$\left[\frac{w_2w_7}{w_6}\right]^2<\frac{w_1}{w_3}\frac{w_2}{w_6}(w_3x^*+w_5)(w_6x^*+w_9) \tag{25c}$$

Proof. The real-valued function $W_4=q_1\int_{x^*}^{x}\frac{u-x^*}{u}du+q_2\int_{y^*}^{y}\frac{v-y^*}{v}dv+q_3\int_{z^*}^{z}\frac{c-z^*}{c}dc$, is defined. By performing direct calculations, it can be shown that $W_4\colon M_4\to\mathbb{R}$, when $M_4=\{(x,y,z)\in\mathbb{R}_+^3\colon x>0,y>0,z>0\}$, holds true. Consequently, this implies $W_4(Q_{xyz})=0$, and $W_4(x,y,z)>0$, for every $(x,y,z)\in M_4-Q_{xyz}$. Furthermore, simple calculations yield that:

$$\frac{dW_4}{dt}=q_1\left(\frac{x-x^*}{x}\right)\frac{dx}{dt}+q_2\left(\frac{y-y^*}{y}\right)\frac{dy}{dt}+q_3\left(\frac{z-z^*}{z}\right)\frac{dz}{dt}.$$

Likewise, employing the concept of maximizing allows for a direct calculation that results in:

$$\frac{dW_4}{dt}=-q_1(x-x^*)^2-q_2[w_3x^*+w_5](y-y^*)^2$$
$$-q_3[w_6x^*+w_9](z-z^*)^2$$
$$-\Big[\frac{q_1w_0}{[1+w_0(y+z)][1+w_0(y^*+z^*)]}+q_1w_1-q_1w_1(y+y^*)$$
$$-q_2w_3(1-y)\Big](x-x^*)(y-y^*)$$
$$-\Big[\frac{q_1w_0}{[1+w_0(y+z)][1+w_0(y^*+z^*)]}+q_1w_2-q_1w_2(z+z^*)$$

$$-q_3 w_6(1-z)](x-x^*)(z-z^*)+q_3 w_7(y-y^*)(z-z^*).$$

By choosing positive constant values as $q_1=1, q_2=\frac{w_1}{w_3}$, and $q_3=\frac{w_2}{w_6}$, the following results are obtained:

$$\frac{dW_4}{dt}=-(x-x^*)^2-\frac{w_1}{w_3}[w_3 x^*+w_5](y-y^*)^2$$

$$-\frac{w_2}{w_6}[w_6 x^*+w_9](z-z^*)^2+\frac{w_2 w_7}{w_6}(y-y^*)(z-z^*)$$

$$-\left[\frac{w_0}{[1+w_0(y+z)][1+w_0(y^*+z^*)]}-w_1 y^*\right](x-x^*)(y-y^*)$$

$$-\left[\frac{w_0}{[1+w_0(y+z)][1+w_0(y^*+z^*)]}-w_2 z^*\right](x-x^*)(z-z^*).$$

Applying the given conditions (25a), (25b) and (25c) leads to the conclusion that:

$$\frac{dW_4}{dt}=-\frac{1}{2}\left[(x-x^*)+\sqrt{\frac{w_1}{w_3}[w_3 x^*+w_5]}(y-y^*)\right]^2$$

$$-\frac{1}{2}\left[(x-x^*)+\sqrt{\frac{w_2}{w_6}[w_6 x^*+w_9]}(z-z^*)\right]^2$$

$$-\frac{1}{2}\left[\sqrt{\frac{w_1}{w_3}[w_3 x^*+w_5]}(y-y^*)-\sqrt{\frac{w_2}{w_6}[w_6 x^*+w_9]}(z-z^*)\right]^2.$$

Note that the derivative $\frac{dW_4}{dt}$ is a negative definite and hence the proof is complete. □

7. LOCAL BIFURCATION

System (2) can be reformulated using Sotomayor's theorem to examine the local bifurcation that may arise near the non-hyperbolic equilibrium point. The objective is to comprehend the impact of parameter variations on the dynamic behavior of the system as the parameter traverses the value that shifts the equilibrium from hyperbolic to non-hyperbolic. Now, let's rephrase system (2) in the following manner.

To rewrite System (2), it is necessary to express it as the derivative of $\mathcal{H}$ concerning t, denoted as $\frac{d\mathcal{H}}{dt}$, which is equal to the function $G(\mathcal{H})$. Here, $\mathcal{H}$ is a column vector $(x,y,z)^T$, and $G(\mathcal{H})$

represents the column vector $(xf_1, yf_2, zf_3)^T$. Consequently, the second directional derivative of the overall Jacobian matrix can be represented in the following manner with the following generic vector $S = (s_1, s_2, s_3)^T$:

$$D^2G(\mathcal{H}).(S,S) = [e_{i1}]_{3\times1} \tag{26}$$

where:

$$\begin{aligned} e_{11} &= -2v_1^2 - \left[\frac{2w_0}{(1+(y+z)w_0)^2} + w_1 + (1-y)w_1 - 3yw_1\right] v_1v_2 \\ &\quad -\left[\frac{2w_0}{(1+(y+z)w_0)^2} + w_2 + (1-z)w_2 - 3zw_2\right] v_1v_3 \\ &\quad +2\left[\frac{w_0^2}{(1+(y+z)w_0)^3}x + w_1x\right] v_2^2 + 4\left[\frac{w_0^2}{(1+(y+z)w_0)^3}x\right] v_2v_3 \\ &\quad +2\left[\frac{w_0^2}{(1+(y+z)w_0)^3} + w_2\right] v_3^2. \\ e_{21} &= -2[w_3x + w_5]v_2^2 - 2[yw_3 - (1-y)w_3]v_1v_2 \\ e_{31} &= -2[xw_6 + w_9]v_3^2 - 2[zw_6 - (1-z)w_6]v_1v_3 + 2w_7v_2v_3 \end{aligned}$$

Theorem 7. If the condition (12a) is satisfied, the system (2) will demonstrate a Transcritical bifurcation near the equilibrium point $Q_1 = (1,0,0)$ if the parameter w_8 passes the value $w_6 = \widetilde{w}_8$.

Proof. The form of the Jacobian matrix for system (2) at Q_1, when w_8 is equal to $\widetilde{w}_8$, can be represented as:

$$H(Q_1, \widetilde{w}_8) = \begin{pmatrix} -1 & -w_1 - w_0 & -w_2 - w_0 \\ 0 & w_3 - w_4 & 0 \\ 0 & 0 & 0 \end{pmatrix} = (d_{ij}).$$

Therefore, the eigenvalues of $H(Q_1, \widetilde{w}_8)$, can be expressed as $\lambda_{11} = -1$, $\lambda_{12} = w_3 - w_4 < 0$ subject to condition (12a), and $\tilde{\lambda}_{13} = 0$.

If we consider $\tilde{S} = (s_{11}, s_{12}, s_{13})^T$ as the eigenvector of $H(Q_1, \widetilde{w}_8)$ corresponding to $\tilde{\lambda}_{13} = 0$, we can derive that $\tilde{S} = (\delta_1 s_{13}, 0, s_{13})^T$, where $s_{13} \neq 0$, $s_{13} \in \mathbb{R}$,

and $\delta_1 = -\frac{d_{13}}{d_{11}} = -(w_2 + w_0) < 0$.

If we consider $\widetilde{\Psi} = (\Psi_{11}, \Psi_{12}, \Psi_{13})^T$, to be the eigenvector of $H(Q_1, \widetilde{w}_8)^T$ associated with $\tilde{\lambda}_{13} = 0$, we can deduce that $\widetilde{\Psi} = (0,0,\Psi_{13})$, is obtained, where $\Psi_{13} \neq 0$ and $\Psi_{13} \in \mathbb{R}$.

Furthermore, by calculating $\frac{\partial G}{\partial w_8} = G_{w_8} = (0,0,-z)^T$, we find that it results in $G_{w_8}(Q_1, \widetilde{w}_8) = (0,0,0)^T$. Consequently, when evaluating $\widetilde{\Psi}^T[G_{w_8}(Q_1, \widetilde{w}_8)] = 0$. Additionally, direct computation demonstrates that:

$$DG_{w_8}(Q_1, \widetilde{w}_8) = \begin{pmatrix} 0 & 0 & 0 \\ 0 & 0 & 0 \\ 0 & 0 & -1 \end{pmatrix} \Longrightarrow DG_{w_8}(Q_x, \widetilde{w}_8)\tilde{S} = (0,0,-s_{13})^T,$$

Subsequently $\dot{\Psi}^T\left[DG_{w_8}(Q_1, \widetilde{w}_8)\tilde{S}\right] = -\Psi_{13}s_{13} \neq 0.$

Upon examining equation (26), it can be noted that

$$\left[D^2G(Q_1, \widetilde{w}_8)\left(\tilde{S}, \tilde{S}\right)\right] = \begin{pmatrix} s_{13}\left[-2{\delta_1}^2 - 2\delta_1 w_0 + 2w_0^2 + 2w_2 - 2\delta_1 w_2\right] \\ 0 \\ s_{13}[-2w_6 + 2\delta_1 w_6 - 2w_9] \end{pmatrix}.$$

thus:

$$\widetilde{\Psi}^T\left[D^2G(Q_1, \widetilde{w}_8)\left(\tilde{S}, \tilde{S}\right)\right] = \Psi_{13}s_{13}(-2w_6 + 2\delta_1 w_6 - 2w_9) \neq 0,$$

Therefore, it can be concluded that a Transcritical bifurcation takes place as per Sotomayor's theorem, and the proof is done. □

Theorem 8. If the condition (15b) is satisfied, the system (2) will demonstrate a Transcritical bifurcation near the equilibrium point $Q_{xy} = (\hat{x}, \hat{y}, 0)$, if the parameter w_8 passes the value $w_6\hat{x} + w_7\hat{y} =: \widehat{w}_8$.

Proof. The form of the Jacobian matrix for system (2) at Q_{xy}, when $w_8 = \widehat{w}_8$, can be represented as:

$$H\left(Q_{xy}, \widehat{w}_8\right) = \begin{bmatrix} -\hat{x} & \hat{x}\left(2w_1\hat{y} - w_1 - \frac{w_0}{(1+w_0\hat{y})^2}\right) & -\hat{x}\left(w_2 + \frac{w_0}{(1+w_0\hat{y})^2}\right) \\ w_3\hat{y}(1-\hat{y}) & -(\mathrm{w}_5 + \mathrm{w}_3\hat{x})\hat{y} & 0 \\ 0 & 0 & 0 \end{bmatrix}.$$

Therefore, the eigenvalues of $H(Q_{xy}, \widehat{w}_8)$, can be expressed as $\lambda_{2i} = \frac{T_{xy}}{2} \pm \frac{1}{2}\sqrt{{T_{xy}}^2 - 4D_{xy}}$, for $i = 1,2$, here λ_{2i} have negative real parts under condition (15b), and $\hat{\lambda}_{23} = 0$.

If we consider $\hat{S} = (s_{21}, s_{22}, s_{23})^T$ as the eigenvector of $H(Q_{xy}, \widehat{w}_8)$ corresponding to $\hat{\lambda}_{23} = 0$, we can derive that $\hat{S} = (\delta_2 s_{23}, \delta_3 s_{23}, s_{23})^T$, where $s_{23} \neq 0$, $s_{23} \in \mathbb{R}$, and $\delta_2 =$

$-\frac{b_{13}b_{22}}{b_{11}b_{22}-b_{12}b_{21}} < 0$, $\delta_3 = \frac{b_{13}b_{21}}{b_{11}b_{22}-b_{12}b_{21}} < 0$, where b_{ij} are the elements of $H(Q_{xy}, \widehat{w}_8)$.

If we consider $\widehat{\Psi} = (\Psi_{21}, \Psi_{22}, \Psi_{23})^T$, to be the eigenvector of $H(Q_{xy}, \widehat{w}_8)^T$ associated with $\hat{\lambda}_{23} = 0$, we can deduce that $\widehat{\Psi} = (0,0,\Psi_{23})$, is obtained, where $\Psi_{23} \neq 0$ and $\Psi_{23} \in \mathbb{R}$. Furthermore, by calculating $\frac{\partial G}{\partial w_8} = G_{w_8} = (0,0,-z)^T$, we find that it results in $G_{w_8}(Q_{xy}, \widehat{w}_8) = (0,0,0)^T$.Consequently, when evaluating $\widehat{\Psi}^T[G_{w_8}(Q_x, \widehat{w}_8)] = 0$. Additionally, direct computation demonstrates that:

$$DG_{w_8}(Q_{xy}, \widehat{w}_8) = \begin{pmatrix} 0 & 0 & 0 \\ 0 & 0 & 0 \\ 0 & 0 & -1 \end{pmatrix} \Longrightarrow DG_{w_8}(Q_{xy}, \widehat{w}_8)\,\hat{S} = (0,0,-s_{23})^T,$$

Subsequently, $\widehat{\Psi}^T\left[\, DG_{w_8}(Q_{xy}, \widehat{w}_8)\,\hat{S}\right] = -\Psi_{23}s_{23} \neq 0$.

Upon examining equation (26), it can be noted that

$$\left[D^2G(Q_{xy}, \widehat{w}_8)\left(\,\hat{S}, \hat{S}\right)\right] = [\hat{e}_{i1}]_{3\times 1},$$

where

$$\hat{e}_{11} = -2{\delta_2}^2{s_{23}}^2 - \left[\frac{2w_0}{(1+\hat{y}w_0)^2} + w_1 + (1-\hat{y})w_1 - 3\hat{y}w_1\right]\delta_2\delta_3{s_{23}}^2$$
$$-\left[\frac{2w_0}{(1+\hat{y}w_0)^2} + w_2 + w_2\right]\delta_2{s_{23}}^2 + 2\left[\frac{w_0^2}{(1+\hat{y}w_0)^3}\hat{x} + w_1\hat{x}\right]{\delta_3}^2{s_{23}}^2$$
$$+4\left[\frac{w_0^2}{(1+\hat{y}w_0)^3}\hat{x}\right]\delta_3{s_{23}}^2 + 2\left[\frac{w_0^2}{(1+\hat{y}w_0)^3} + w_2\right]{s_{23}}^2$$
$$\hat{e}_{21} = -2[w_3\hat{x} + w_5]{\delta_3}^2{s_{23}}^2 - 2[\hat{y}w_3 - (1-\hat{y})w_3]\delta_2\delta_3{s_{23}}^2$$
$$\hat{e}_{31} = -2[\hat{x}w_6 + w_9]{s_{23}}^2 + 2w_6\delta_2{s_{23}}^2 + 2w_7\delta_3{s_{23}}^2 \;.$$

Thus:

$$\widehat{\Psi}^T\left[D^2G\left(Q_{xy}, \widehat{w}_8\right)\left(\,\hat{S}, \hat{S}\right)\right] =$$
$$\Psi_{13}(-2(\hat{x}w_6 + w_9){s_{23}}^2 + 2w_6\delta_2{s_{23}}^2 + 2w_7\delta_3{s_{23}}^2) \neq 0,$$

It can be concluded that a Transcritical bifurcation occurs near Q_{xy} when $w_8 = \widehat{w}_8$. □

Theorem 9. If the condition (18b) is satisfied, the system (2) will demonstrate a Transcritical bifurcation near the equilibrium point $Q_{xz} = (\bar{x}, 0, \bar{z})$, when the parameter w_4 passes the value $w_3\bar{x} =: \overline{w}_4$ provided that the following condition holds:

$$-2\bar{x}w_3 - 2w_5 + 2w_3\delta_5 \neq 0. \tag{27}$$

Proof. The form of the Jacobian matrix for system (2) at Q_{xz}, when $\overline{w}_4 = w_3\bar{x}$, can be represented as:

$$H(Q_{xz}, \overline{w}_4) = \begin{bmatrix} -\bar{x} & -\bar{x}\left(w_1 + \frac{w_0}{(1+w_0\bar{z})^2}\right) & \bar{x}\left(2w_2\bar{z} - w_2 - \frac{w_0}{(1+w_0\bar{z})^2}\right) \\ 0 & 0 & 0 \\ w_6\bar{z} - w_6\bar{z}^2 & w_7\bar{z} & -w_9\bar{z} - w_6\bar{x}\bar{z} \end{bmatrix}.$$

Therefore, the eigenvalues of $H(Q_{xz}, \overline{w}_4)$, can be expressed as $\lambda_{3i} = \frac{T_{xz}}{2} \pm \frac{1}{2}\sqrt{{T_{xz}}^2 - 4D_{xz}}$, for $i = 1,3$ which have negative real parts provided that condition (18b) holds, and $\bar{\lambda}_{32} = 0$.

If we consider $\bar{S} = (s_{31}, s_{32}, s_{33})^T$ as the eigenvector of $H(Q_{xz}, \overline{w}_4)$ corresponding to$\bar{\lambda}_{32} = 0$, we can derive that $\bar{S} = (\delta_5 s_{32}, s_{32}, \delta_4 s_{32})^T$, where $s_{32} \neq 0$, $s_{32} \in \mathbb{R}$, and $\delta_4 = \frac{c_{13}c_{32} - c_{33}c_{12}}{c_{11}c_{33} - c_{13}c_{31}}$, and $\delta_5 = \frac{c_{12}c_{31} - c_{11}c_{32}}{c_{11}c_{33} - c_{13}c_{31}} > 0$, where c_{ij} are the elements of $H(Q_{xz}, \overline{w}_4)$.

If we consider $\bar{\Psi} = (\Psi_{31}, \Psi_{32}, \Psi_{33})^T$, to be the eigenvector of $H(Q_{xz}, \overline{w}_4)^T$ associated with $\bar{\lambda}_{32} = 0$, we can deduce that $\bar{\Psi} = (0, \Psi_{32}, 0)$, is obtained, where $\Psi_{32} \neq 0$ and $\Psi_{32} \in \mathbb{R}$.

Furthermore, by calculating $\frac{\partial G}{\partial w_4} = G_{w_4} = (0, -y, 0)^T$, we find that it results in $G_{w_4}(Q_{xz}, \overline{w}_4) = (0,0,0)^T$. Consequently, when evaluating $\bar{\Psi}^T[G_{w_4}(Q_{xz}, \overline{w}_4)] = 0$. Additionally, direct computation demonstrates that:

$$DG_{w_4}(Q_{xz}, \overline{w}_4) = \begin{pmatrix} 0 & 0 & 0 \\ 0 & -1 & 0 \\ 0 & 0 & 0 \end{pmatrix} \Longrightarrow DH_{w_4}(Q_{xz}, \overline{w}_4)\,\bar{S} = (0, -s_{32}, 0)^T.$$

Subsequently $\bar{\Psi}^T\left[DG_{w_4}(Q_{xz}, \overline{w}_4)\bar{S}\right] = -\Psi_{32}s_{32} \neq 0$.

Upon examining equation (26), it can be noted that

$[D^2G(Q_{xz}, \overline{w}_4)(\bar{S}, \bar{S})] = [\bar{e}_{i1}]_{3\times 1}$, where:

$$\bar{e}_{11} = s_{32}^2\Big(\frac{2\bar{x}w_0^2}{(1+\bar{z}w_0)^3} + 2xw_1 + \frac{4\bar{x}w_0^2\delta_4}{(1+\bar{z}w_0)^3} + \frac{2\bar{x}w_0^2\delta_4^2}{(1+\bar{z}w_0)^3} + 2\bar{x}w_2\delta_4^2 - \frac{2w_0\delta_5}{(1+\bar{z}w_0)^2}$$
$$- 2w_1\delta_5 - \frac{2w_0\delta_4\delta_5}{(1+\bar{z}w_0)^2} - w_2\delta_4\delta_5 + (-1+\bar{z})w_2\delta_4\delta_5 + 3zw_2\delta_4\delta_5 - 2\delta_5^2\Big),$$

$$\bar{e}_{21} = s_{32}^2(-2\bar{x}w_3 - 2w_5 + 2w_3\delta_5),$$

$$\bar{e}_{31} = s_{32}^2(2w_7\delta_4 - 2\bar{x}w_6\delta_4^2 - 2w_9\delta_4^2 + 2(1-\bar{z})w_6\delta_4\delta_5 - 2\bar{z}w_6\delta_4\delta_5).$$

thus:

$$\bar{\Psi}^T[D^2G(Q_{xz},\bar{w}_4)(\bar{S},\bar{S})] = \Psi_{32}s_{32}^2(-2\bar{x}w_3 - 2w_5 + 2w_3\delta_5),$$

Therefore, due to condition (27), it can be concluded that a Transcritical bifurcation occurs near Q_{xz} when $\bar{w}_4 = w_3\bar{x}$. □

Theorem 10. If the conditions (18a)-(18d) are met, the transition of the parameter w_5 from a positive value w_5^* causes the system (2) to experience a saddle-node bifurcation near the coexistence equilibrium point Q_{xyz} if the following condition holds.

$$\delta_7 e^*_{11} + \delta_8 e^*_{21} + e^*_{31} \neq 0, \tag{28}$$

where all the new symbols are defined in the proof, while w_5^* is given by.

$$w_5^* = \frac{a_{13}a_{21}a_{32} - a_{12}a_{21}a_{33}}{y^*(a_{11}a_{33} - a_{13}a_{31})} - w_3x^*. \tag{29}$$

Proof. The form of the Jacobian matrix for system (2) at Q_{xyz}, when $w_5 = w_5^*$, can be represented as:

$$H_5 = H\left(Q_{xyz}, w_5^*\right) = [a_{ij}],$$

where a_{ij} for all $i,j = 1,2,3$ are given in eqution (20) with $a_{22}(w_5^*) = -(w_5^* + w_3x^*)y^*$.
Therefore, direct computation shows that the coefficient $C = 0$ in the characteristic equation (21).
Thus, equation (21) has a zero root represented by $\lambda_{43}^* = 0$, and two other eigenvalues have negative real parts under the conditions (18a)-(18b).

Consider now $S^* = (s_{41}, s_{42}, s_{43})^T$ as the eigenvector of H_5 corresponding to $\lambda_{43}^* = 0$, we can derive that $S^* = (\delta_5 s_{43}, \delta_6 s_{43}, s_{42})^T$, where $s_{43} \neq 0$, $s_{43} \in \mathbb{R}$,
with $\delta_5 = -\frac{a_{13}a_{22}}{a_{11}a_{22} - a_{12}a_{21}}$ and $\delta_6 = \frac{a_{13}a_{21}}{a_{11}a_{22} - a_{12}a_{21}}$

Moreover, consider $\Psi^* = (\Psi_{41}, \Psi_{42}, \Psi_{43})^T$, to be the eigenvector of ${H_5}^T$ associated with $\lambda_{43}^* = 0$, we can deduce that $\Psi^* = (\delta_7\Psi_{43}, \delta_8\Psi_{43}, \Psi_{43})$, where $\Psi_{43} \neq 0$ and $\Psi_{43} \in \mathbb{R}$ with $\delta_7 = \frac{a_{21}a_{32} - a_{22}a_{31}}{a_{11}a_{22} - a_{12}a_{21}}$ and $\delta_8 = \frac{a_{12}a_{31} - a_{11}a_{32}}{a_{11}a_{22} - a_{12}a_{21}}$

Furthermore, by calculating $\frac{\partial G}{\partial w_5} = G_{w_5} = (0, -y^2, 0)^T$, we find that it results in

$G_{w_5}\left(Q_{xyz}, w_5^*\right) = (0, -(y^*)^2, 0)^T$.

Consequently, when evaluating $\Psi^{*T}\left[G_{w_5}(Q_{xz}, w_5^*)\right] = -\delta_8 \Psi_{43}(y^*)^2 \neq 0$. Thus the first condition of the occurrence of a SNB is satisfied. Additionally, direct computation demonstrates that.Upon examining equation (26), it can be noted that

$$\left[D^2 G(Q_{xyz}, w_5^*)(\, S^*, S^*)\right] = [e_{i1}^*]_{3\times 1},$$

where:

$$e_{11}^* = -2(\delta_5 s_{43})^2 - \left[\frac{2w_0}{\left(1+w_0(y^*+z^*)\right)^2} + 2w_1(1-2y^*)\right]\delta_5\delta_6 {s_{43}}^2$$
$$-\left[\frac{2w_0}{\left(1+w_0(y^*+z^*)\right)^2} + 2w_2(1-2z^*)\right]\delta_5 {s_{43}}^2 + 4\left[\frac{w_0^2 x^*}{\left(1+w_0(y^*+z^*)\right)^3}\right]\delta_6 {s_{43}}^2$$
$$+2x^*\left[\frac{w_0^2}{\left(1+w_0(y^*+z^*)\right)^3} + w_1\right](\delta_6 s_{43})^2 + 2\left[\frac{w_0^2}{(1+w_0(y^*+z^*))^3} + w_2\right]{s_{43}}^2,$$
$$e_{21}^* = -2[w_3 x^* + w_5](\delta_6 s_{43})^2 - 2w_3[2y^* - 1]\delta_5\delta_6 {s_{43}}^2,$$
$$e_{31}^* = -2[w_6 x^* + w_9]{s_{43}}^2 - 2w_6[2z^* - 1]v_1 v_3 + 2w_7\delta_6 {s_{43}}^2 \; .$$

Thus, due to condition (28), it is obtained that:

$$\Psi^{*T}\left[D^2 G(Q_{xyz}, w_5^*)(\, S^*, S^*)\right] = [\delta_7 {e^*}_{11} + \delta_8 {e^*}_{21} + {e^*}_{31}]\Psi_{43} \neq 0,$$

Therefore, it can be concluded that a saddle-node bifurcation occurs near Q_{xyz}. □

8. PERSISTENCE

In this division, we delve into the examination of the persistence of the system (2). Acknowledging that the system is considered to persist only if and only if none of its species becomes extinct is crucial. This implies that system (2) persists if the trajectory of the system, starting from a positive initial point, does not approach the boundary planes of its domain as its omega limit set.

System (2) consists of two subsystems positioned within the $xy-plane$ and $xz-plane$, respectively. The representation of these subsystems is as follows for each plane.

$$\frac{dx}{dt} = x\left[\frac{1}{1+w_0 y} - x - w_1(1-y)y\right] = t_1(x, y), \tag{30}$$

$$\frac{dy}{dt} = y[w_3(1-y)x - w_4 - w_5 y] = t_2(x,y),$$

And

$$\frac{dx}{dt} = x\left[\frac{1}{1+w_0 z} - x - w_2(1-z)z\right] = t_3(x,z), \tag{31}$$

$$\frac{dz}{dt} = z[w_6(1-z)x - w_8 - w_9 z] = t_4(x,z),$$

To explore the presence of periodic dynamics in the $Int.\mathbb{R}^2_+$ of the $xy-plane$, we can establish the Dulac function as $q_1(x,y) = \frac{1}{xy}$ which fulfills the criteria outlined by the $q_1(x,y) > 0$ and C^1 functions. Consequently, we can deduce that

$$q_1 t_1 = \frac{1}{y}\left[\frac{1}{1+w_0 z} - x - w_2(1-z)z\right],$$

And

$$q_1 t_2 = \frac{1}{x}[w_3(1-y)x - w_4 - w_5 y]$$

Therefore, it can be concluded that:

$$\Delta(x,y) = \frac{\partial(q_1 t_1)}{\partial x} + \frac{\partial(q_1 t_2)}{\partial y} = -(w_3 + \frac{1}{y} + \frac{w_5}{x})$$

Because the value of $\Delta(x,y)$ is not consistently zero and does not exhibit a change in sign within $Int.\mathbb{R}^2_+$ of the $xy-plane$, the Dulac-Bendixon criterion indicates that the system (30) lacks any periodic solution that exists exclusively within the interior of the $xy-plane$.

Likewise, it is straightforward to confirm that the system (31) does not exhibit any periodic solution that exists exclusively within the interior of the $xz-plane$ by employing the Dulac function $q_2(x,z) = \frac{1}{xz}$ for verification.

Theorem 11. If there are no recurring patterns in the boundary planes, the system (2) will exhibit uniform persistence as long as the following conditions are satisfied.

$$w_3 > w_4, \tag{32a}$$

$$w_6 > w_8, \tag{32b}$$

$$\hat{x} > \frac{w_8 - w_7\hat{y}}{w_6}, \tag{32c}$$

$$\bar{x} > \frac{w_4}{w_3}. \tag{32d}$$

Proof. Define the function $\sigma(x, y, z) = x^{\eta_1} y^{\eta_2} z^{\eta_3}$, using the average Lyapunov function approach, where $\eta_i, \forall i = 1,2,3$, represents positive constants.

Consequently, $\sigma(x, y, z) > 0$, holds for all $(x, y, z) \in int.\mathbb{R}^3_+$ and $\sigma(x, y, z) \to 0$, when any of their variables approaches zero. Consequently, it can be concluded that

$$\Omega(x, y, z) = \frac{\sigma'(x,y,z)}{\sigma(x,y,z)} = \eta_1 \left[\frac{1}{1+w_0(y+z)} - x - w_1(1-y)y - w_2(1-z)z\right]$$
$$+\eta_2[w_3(1-y)x - w_4 - w_5 y] + \eta_3[w_6(1-z)x + w_7 y - w_8 - w_9 z].$$

Based on the average Lyapunov function, the proof is completed when $\Omega(Q) > 0$ holds for any attractor point Q on the boundary planes, given an appropriate choice of constants $\eta_i > 0$, $j = 1,2,3$. Since

$$\Omega(Q_0) = \eta_1 - \eta_2 w_4 - \eta_3 w_8,$$
$$\Omega(Q_x) = \eta_2(w_3 - w_4) + \eta_3(w_6 - w_8),$$
$$\Omega(Q_{xy}) = \eta_3[w_6\hat{x} + w_7\hat{y} - w_8].$$
$$\Omega(Q_{xz}) = \eta_2[w_3\bar{x} - w_4].$$

By choosing a suitably large value for η_1, $\Omega(Q_0) > 0$ can be achieved. However, $\Omega(Q_1) > 0$, $\Omega(Q_{xy}) > 0$, and $\Omega(Q_{xz}) > 0$, are only possible if conditions (32a), (32b), (32c), and (32d) are satisfied. Therefore, the proof is concluded. □

9. NUMERICAL SIMULATION

In this section, we use methods to explore the behavior of system (2) and confirm the analytical findings. We also determine the control parameters that're appropriate, for the system by solving it with a hypothetical set of values. By representing the resulting trajectories through time series plots and phase portrait we can thoroughly analyze how the system behaves. This analysis helps us validate our results and identify values, for the control parameters.

Table 2. Data of parameter values.

w_0	w_1	w_2	w_3	w_4	w_5	w_6	w_7	w_8	w_9
0.6	0.5	0.6	0.49	0.28	0.3	0.4	0.4	0.2	0.3

The analysis of the given table (2) reveals that system (2) possesses a globally asymptotically stable positive equilibrium point at coordinates $Q_{xyz} = (0.71, 0.1, 0.21)$. This finding is visually depicted in Figure 1-2, confirming the stability of the equilibrium point.

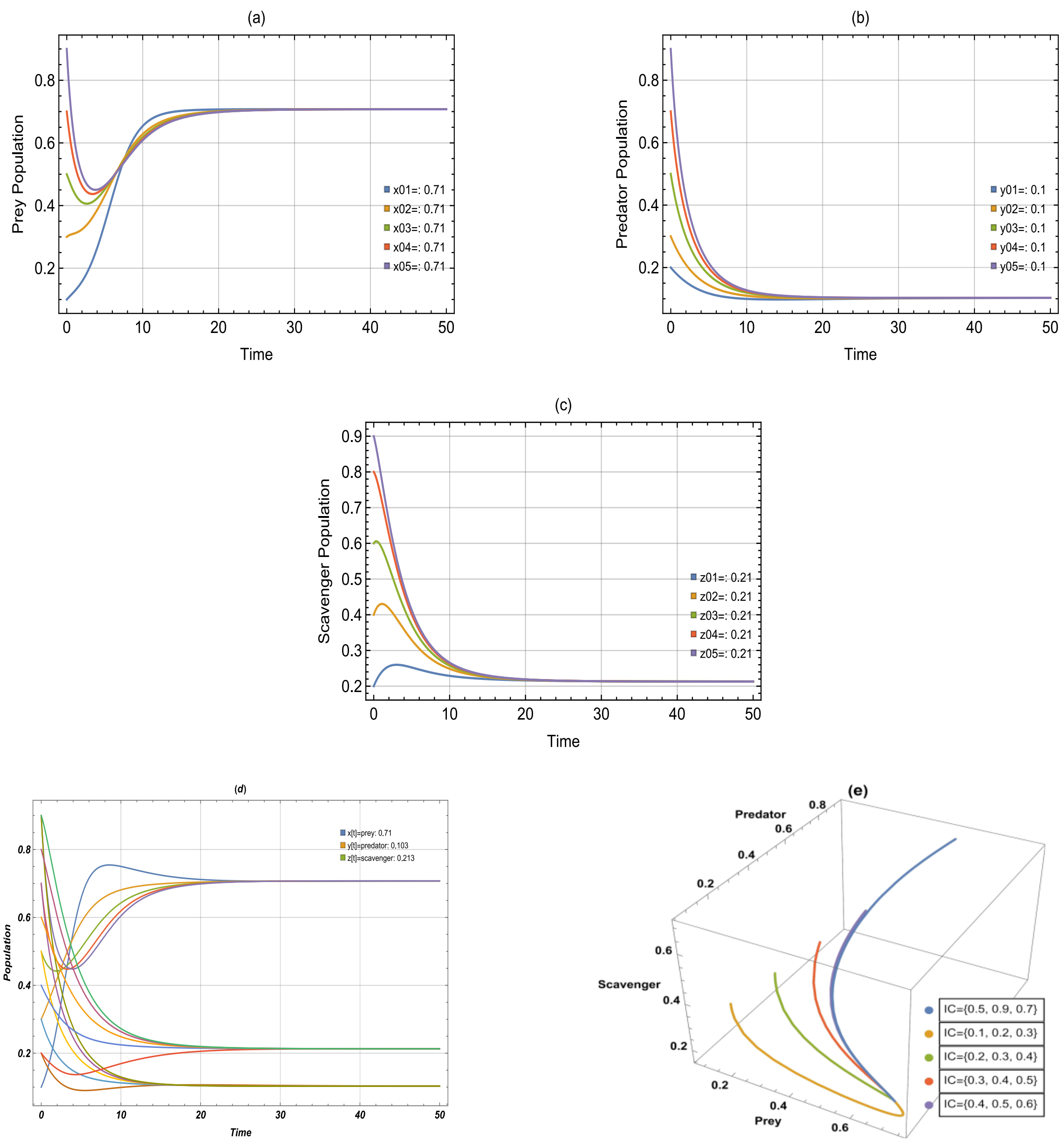

Figure 1. The trajectories of the system (2) by utilizing table (2) and starting from different initial points. (a) The trajectories showcase the motion exhibited by the prey versus time. (b) The trajectories showcase the motion exhibited by a predator versus time. (c) The trajectories showcase the motion exhibited by scavengers versus time. (d) Time series for the trajectories prey, predator, and scavenger of the system (2). (e) 3D-Phase portrait of the system (2).

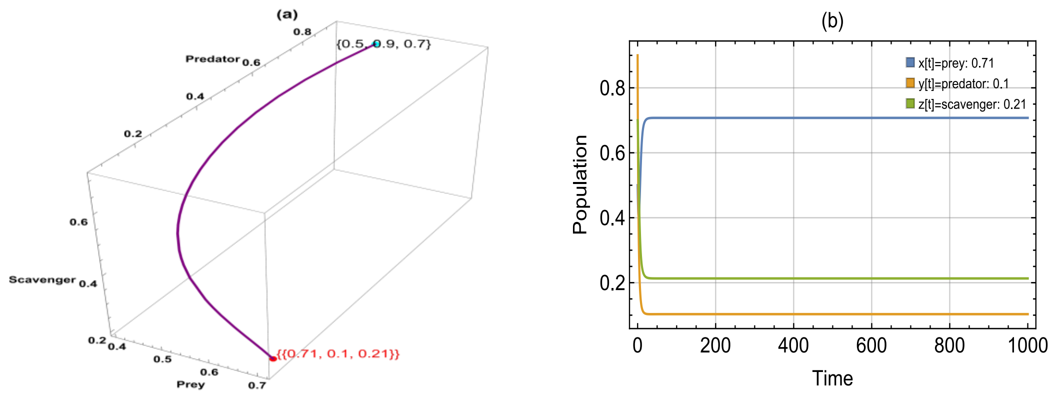

Figure 2. (a) 3D-Phase portrait of the system (2). (b)The time series exhibits the trajectories of the system (2) by utilizing table (2), the trajectories of three species demonstrate an asymptotic positive convergence towards $Q_{xyz} = (0.71, 0.1, 0.21)$.

To explore the influence of parameter variations on the dynamics of the system (2), numerical solutions are obtained by systematically varying one parameter at a time. The resulting trajectories are then analyzed to identify the attractors, which are depicted in Figures (3–9) for visual reference. This approach allows for a comprehensive understanding of how changes in parameter values affect the behavior of the system. Upon examination of the given table (2) and considering the value of $12 \leq w_0 < 25$, it is apparent that the trajectory of the system (2) demonstrates an asymptotic convergence towards a predator-free equilibrium point, see Figure (3). Conversely, in all other cases for $0 < w_0 < 12$, the trajectory asymptotically approaches a positive equilibrium point.

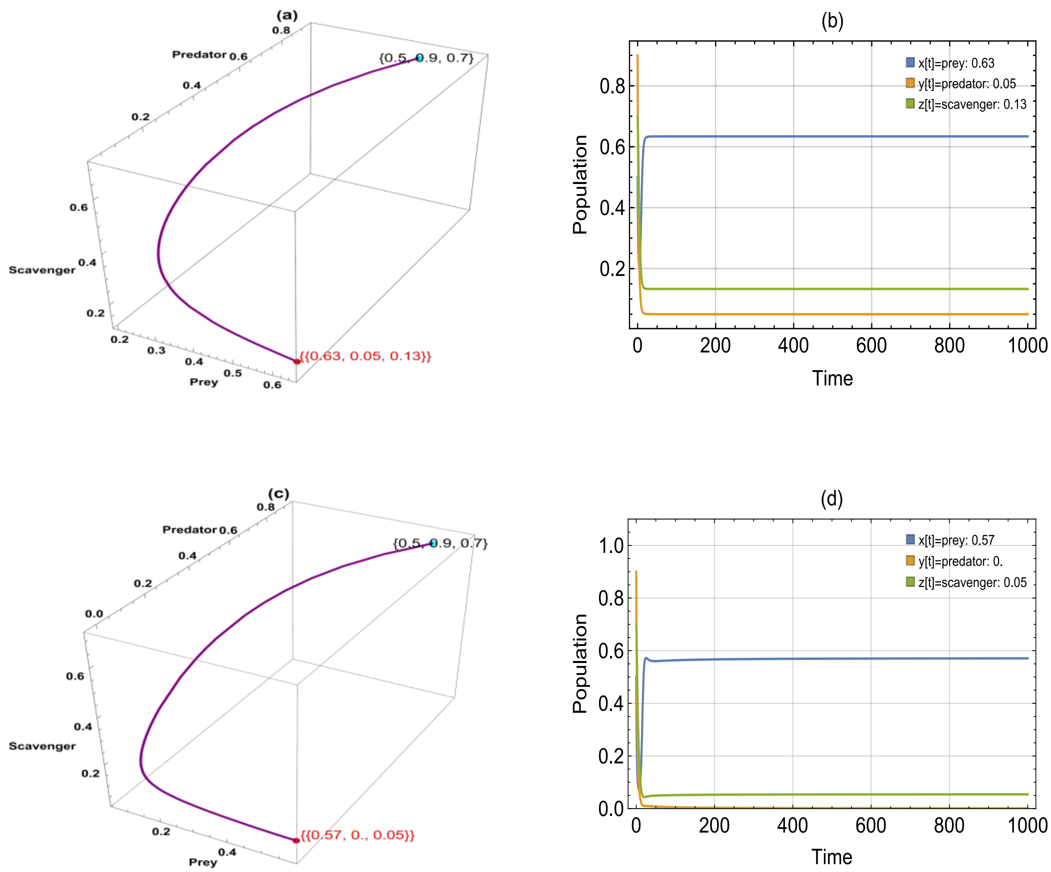

Figure 3. The trajectories of the system (2) by utilizing table (2) with values of w_0. (a) 3D-Phase portrait when $w_0 = 2$. (b) Time series for the trajectories when $w_0 = 2$. (c) 3D-Phase portrait when $w_0 = 12$. (d) Time series for the trajectories when $w_0 = 12$.

When the value of w_1 increases, the impact it has on the predator becomes evident. This is observed when $w_1 = 1.9$. In such instances, a decline in the predator population is noticed compared to the previous value, see Figure (4).

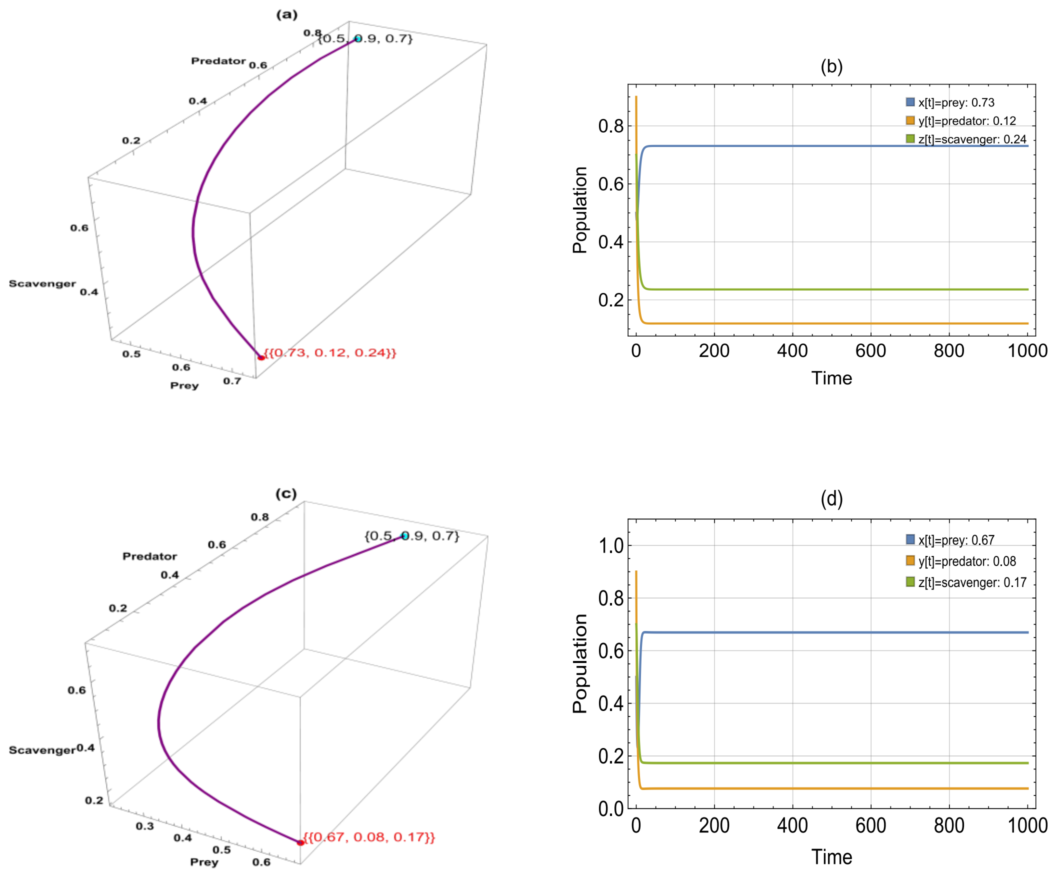

Figure 4. The trajectories of the system (2) by utilizing table (2) with different values of w_1. (a) 3D-Phase portrait when $w_1 = 0.1$. (b) Time series for the trajectories when $w_1 = 0.1$. (c) 3D-Phase portrait when $w_1 = 1.9$. (d) Time series for the trajectories when $w_1 = 1.9$.

However, when the value of w_2 increases, the impact it has on the scavenger becomes evident. This is observed when $w_2 = 1.9$. In such instances, a decline in the scavenger population is noticed compared to the previous value, see Figure (5).

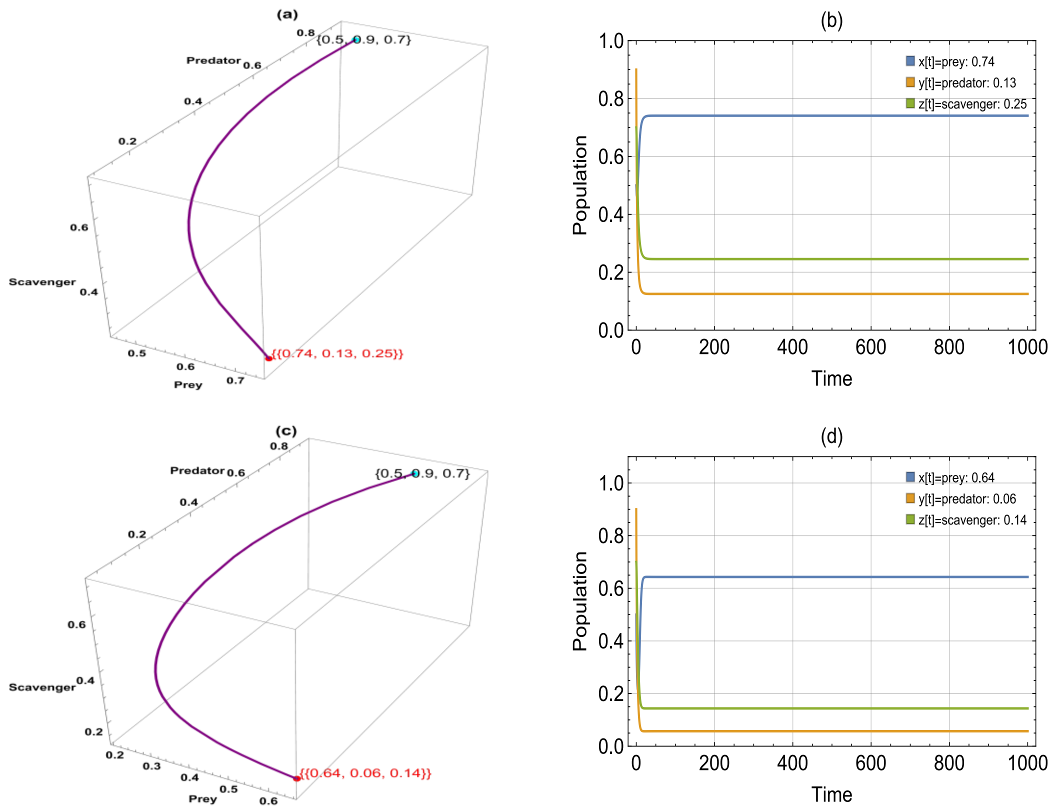

Figure 5. The trajectories of the system (2) by utilizing table (2) with different values of w_2. (a) 3D-Phase portrait when $w_2 = 0.2$. (b) The time series of the trajectories when $w_2 = 0.2$. (c) 3D-Phase portrait when $w_2 = 1.9$. (d) The time series of the trajectories when $w_2 = 1.9$.

Alternatively, in the case of table (2) with $0 < w_3 \leq 0.34$, the solution of system (2) gradually converges asymptotically $Q_{xz} = (\bar{x}, 0, \bar{z})$ as depicted in the Figures (6). Conversely, for $0.34 < w_3 < 1$ the system maintains a globally asymptotically stable positive equilibrium point.

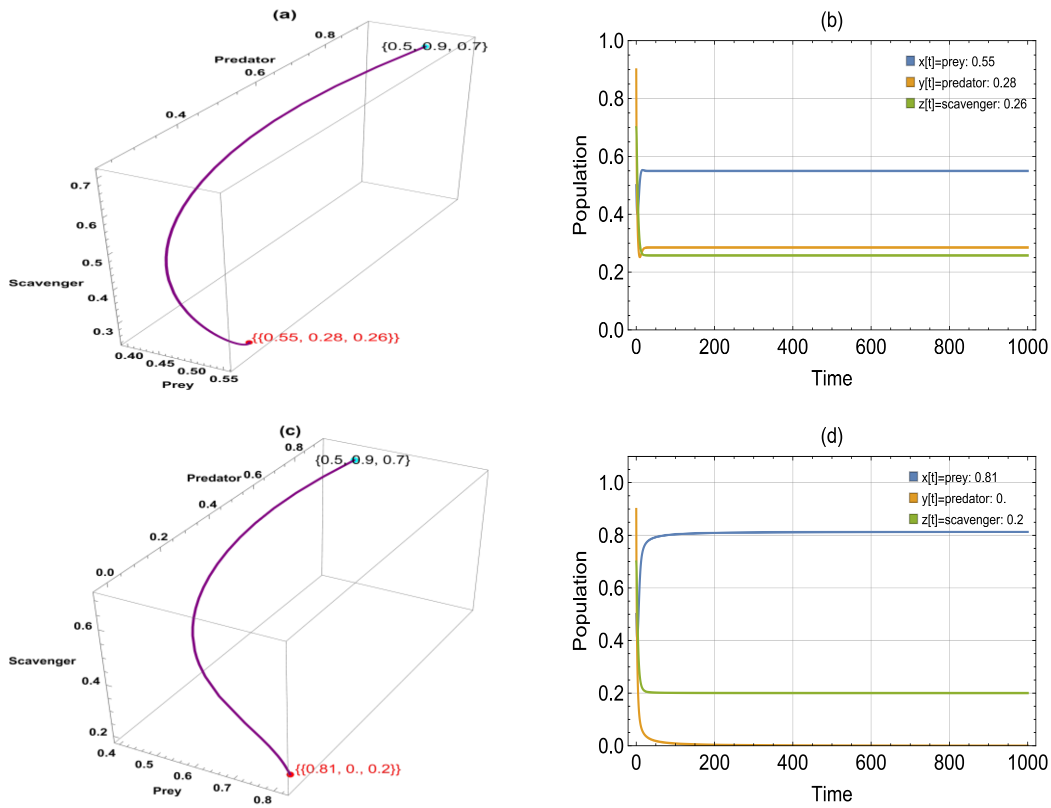

Figure 6. The trajectories of the system (2) by utilizing table (2) with different values of w_3. (a) 3D-Phase portrait when $w_3 = 0.93$. (b) The time series of the trajectories when $w_3 = 0.93$. (c) 3D-Phase portrait when $w_3 = 0.34$. (d) The time series of the trajectories when $w_3 = 0.34$.

In the case of the parameters table (2) with $0.4 \leq w_4 < 1$, the trajectory of the system (2) demonstrates asymptotic convergence towards $Q_{xz} = (\bar{x}, 0, \bar{z})$ as illustrated in Figure (7). However, for $0 < w_4 < 0.4$ the system maintains a globally asymptotically stable positive point.

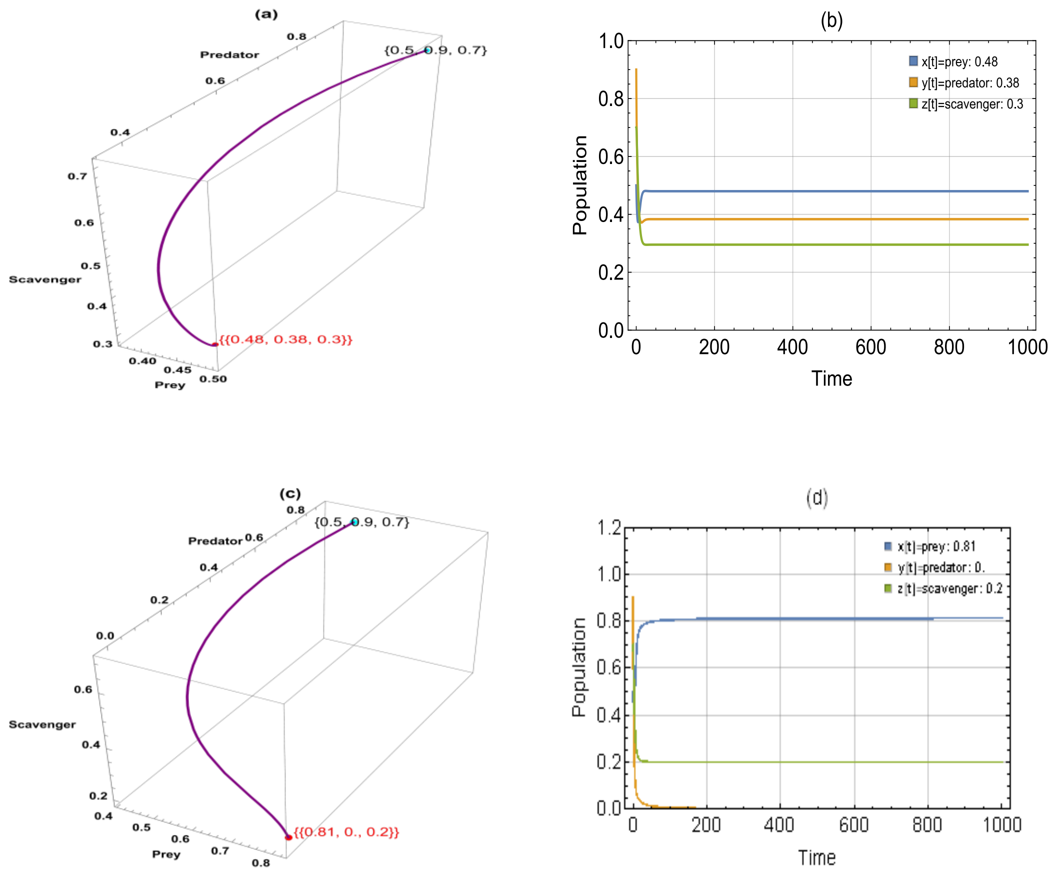

Figure 7. The trajectories of the system (2) by utilizing table (2) with different values of w_4. (a) 3D-Phase portrait when $w_4 = 0.03$. (b) The time series of the trajectories when $w_4 = 0.03$. (c) 3D-Phase portrait when $w_4 = 0.4$. (d) The time series of the trajectories when $w_4 = 0.4$.

Furthermore, it is noted that when the parameter w_5 is varied while keeping the rest of the parameters as table (2), it has a quantitative impact on the dynamics of the system (2). The solution of the system continues to converge towards a positive equilibrium point, which is dependent on the value of w_5. Now, considering the specific parameter values provided by table (2) with $0 < w_6 \leq 0.153$, the trajectory of the system (2) asymptotically approaches $Q_{xy} = (\hat{x}, \hat{y}, 0)$. This behavior is depicted in Figure (8). Conversely, for $0.153 < w_6 < 1$ the system remains stable at a positive equilibrium point.

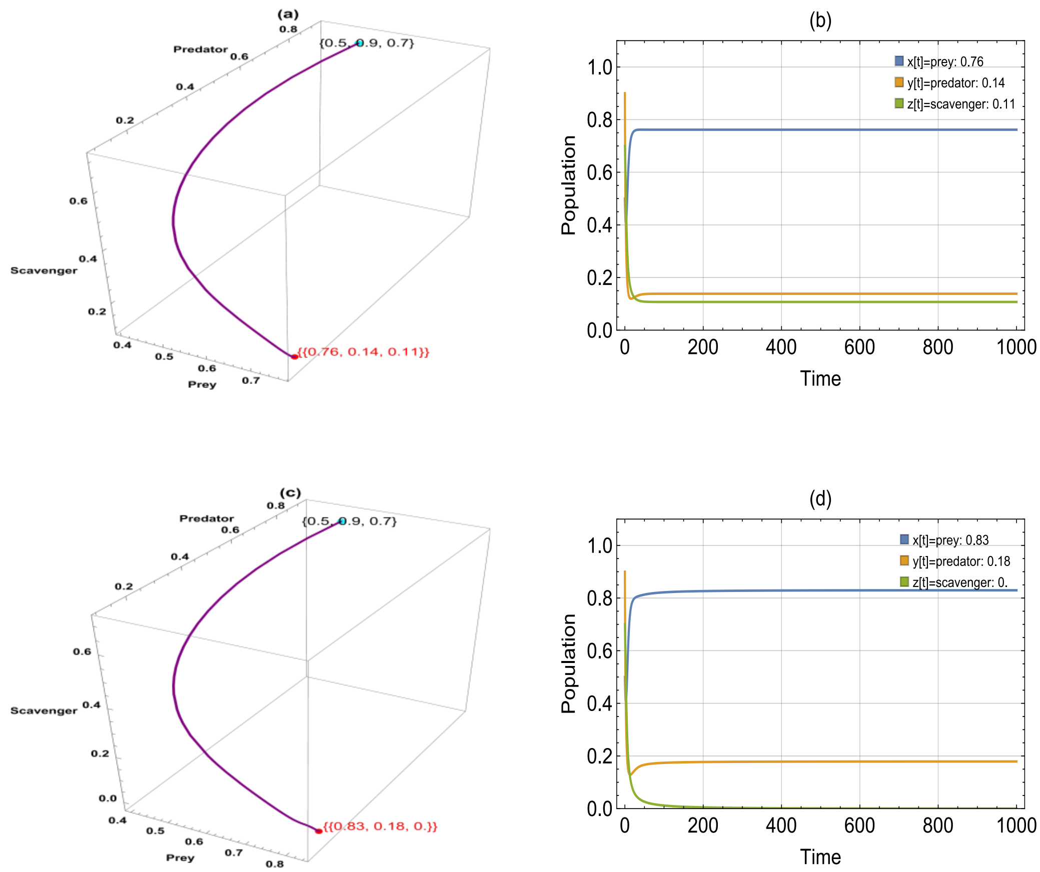

Figure 8. The trajectories of the system (2) by utilizing table (2) with different values of w_6. (a) 3D-Phase portrait when $w_6 = 0.26$. (b) The time series of the trajectories when $w_6 = 0.26$. (c) 3D-Phase portrait when $w_6 = 0.15$. (d) The time series of the trajectories when $w_6 = 0.15$.

Finally, it is noted that when the parameter w_7 (similary as w_9) is varied while keeping the rest of the parameters as table (2) , it has a quantitative impact on the dynamics of the system (2). The solution of the system continues to converge towards a positive equilibrium point, which is dependent on the value of w_7. Now, considering the specific parameter values provided by table (2) with $0.41 \leq w_8 < 1$, the trajectory of the system (2) asymptotically approaches $Q_{xy} = (\hat{x}, \hat{y}, 0)$. This behavior is depicted in Figure (9). Conversely, for $0 < w_8 < 0.41$ the system remains stable at a positive equilibrium point.

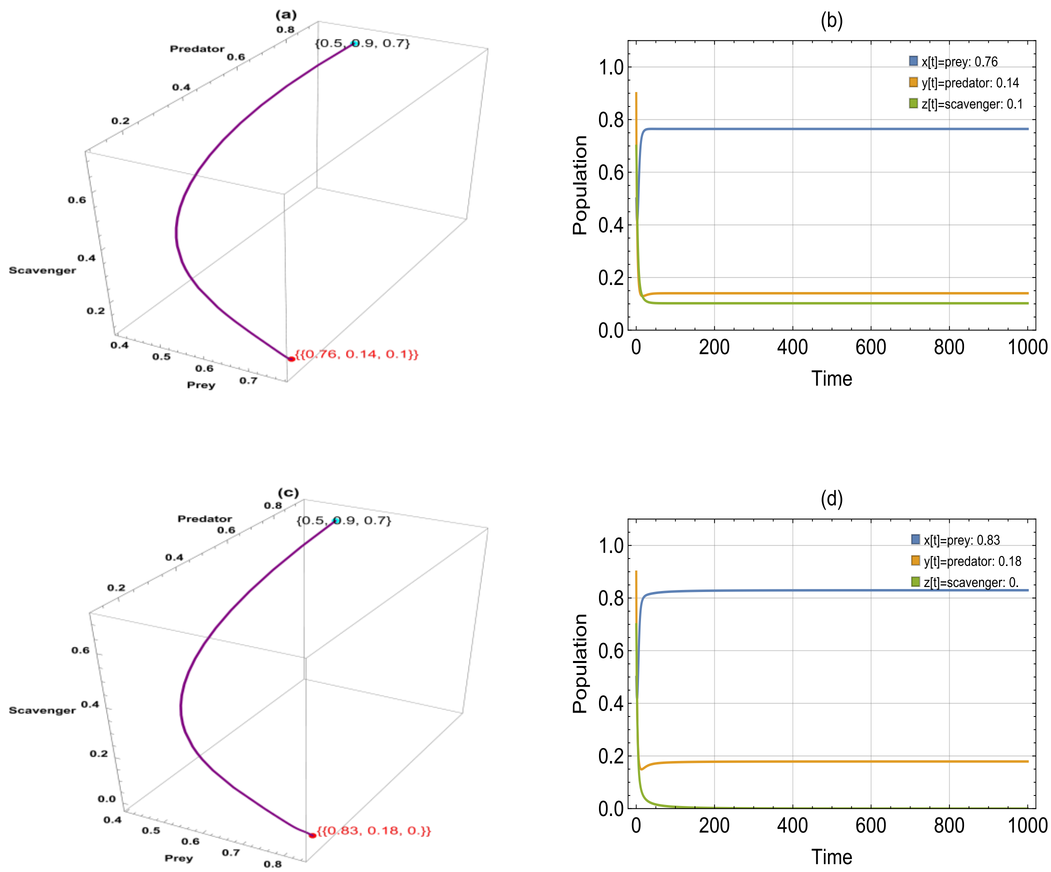

Figure 9. The trajectories of the system (2) by utilizing table (2) with different values of w_8. (a) 3D-Phase portrait when $w_8 = 0.3$. (b) The time series of the trajectories when $w_8 = 0.3$. (c) 3D-Phase portrait when $w_8 = 0.41$. (d) The time series of the trajectories when $w_8 = 0.41$.

10. CONCLUSIONS

A mathematical structure of an ecological system with a prey-predator-scavenger dynamic in the presence of fear and predator-dependent refuge has been made. We go over every property of the solution. The local stability of the equilibrium points is examined. The requirements for persistence have been determined. The Sotomayor theorem is used to study all potential local bifurcations. Several Lyapunov functions are proposed to investigate the system's global stability. Finally, numerical simulation has been utilized using a proposed hypothetical set of biologically feasible data given by table (2) to validate our findings. The Mathematica program was used to obtain all of the numerical findings, which are all described below.

The system (2) approaches asymptotically to the coexistence equilibrium point, starting from different initial points, indicating the possibility of global stability at this point. The investigation of the influence of altering the parameter's value indicates that the parameters are divided into three compartments depending on the table (2). The parameters in the first compartment work as a stabilizing set and those are given by the growth rates of the predator and scavenger, respectively, due to the feeding on the prey. The parameters in the second compartment work as a destabilizing set of parameters, causing extinction in either predator or scavenger, that consist of the fear level and the death rates of the predator and scavenger, respectively. All other parameters, including the feeding rate of the scavenger on the predator's carcass and those parameters related to the harvesting, belong to the third compartment and have quantitative effects on the position of the coexistence point.

CONFLICT OF INTERESTS

The authors declare that there is no conflict of interests.

REFERENCES

[1] A.A. Berryman, The orgins and evolution of predator-prey theory, Ecology 73 (1992), 1530-1535. https://doi.org/10.2307/1940005.

[2] Y. Kuang, E. Beretta, Global qualitative analysis of a ratio-dependent predator-prey system, J. Math. Biol. 36 (1998), 389-406. https://doi.org/10.1007/s002850050105.

[3] T.K. Kar, Stability analysis of a prey–predator model incorporating a prey refuge, Commun. Nonlinear Sci. Numer. Simul. 10 (2005), 681-691. https://doi.org/10.1016/j.cnsns.2003.08.006.

[4] Y. Huang, F. Chen, L. Zhong, Stability analysis of a prey–predator model with holling type III response function incorporating a prey refuge, Appl. Math. Comput. 182 (2006), 672-683. https://doi.org/10.1016/j.amc.2006.04.030.

[5] H. Merdan, Stability analysis of a Lotka-Volterra type predator-prey system involving Allee effects, ANZIAM J. 52 (2010), 139-145. https://doi.org/10.1017/s1446181111000630.

[6] J. Wang, L. Pan, Qualitative analysis of a harvested predator-prey system with Holling-type III functional response incorporating a prey refuge, Adv. Differ. Equ. 2012 (2012), 96. https://doi.org/10.1186/1687-1847-2012-96.

[7] Yusrianto, S. Toaha, Kasbawati, Stability analysis of prey predator model with Holling II functional response and threshold harvesting for the predator, J. Phys.: Conf. Ser. 1341 (2019), 062025. https://doi.org/10.1088/1742-6596/1341/6/062025.

[8] N.H. Fakhry, R.K. Naji, The dynamics of a square root prey-predator model with fear, Iraqi J. Sci. 61 (2020), 139-146. https://doi.org/10.24996/ijs.2020.61.1.15.

[9] S. Al-Momen, R.K. Naji, The dynamics of Sokol-Howell prey-predator model involving strong Allee effect, Iraqi J. Sci. 62 (2021), 3114–3127. https://doi.org/10.24996/ijs.2021.62.9.27.

[10] A. Hastings, T. Powell, Chaos in a three-species food chain, Ecology 72 (1991), 896-903. https://doi.org/10.2307/1940591.

[11] M.C. Varriale, A.A. Gomes, A study of a three species food chain, Ecol. Model. 110 (1998), 119-133. https://doi.org/10.1016/s0304-3800(98)00062-3.

[12] S. Lv, M. Zhao, The dynamic complexity of a three species food chain model, Chaos Solitons Fractals 37 (2008), 1469-1480. https://doi.org/10.1016/j.chaos.2006.10.057.

[13] P. Panday, N. Pal, S. Samanta, et al. Stability and bifurcation analysis of a three-species food chain model with fear, Int. J. Bifurcation Chaos 28 (2018), 1850009. https://doi.org/10.1142/s0218127418500098.

[14] H.A. Ibrahim, R.K. Naji, The complex dynamic in three species food webmodel involving stage structure and cannibalism, AIP Conf. Proc. 2292 (2020), 020006. https://doi.org/10.1063/5.0030510.

[15] F.H. Maghool, R.K. Naji, Chaos in the three-species Sokol-Howell food chain system with fear, Commun. Math. Biol. Neurosci. 2022 (2022), 14. https://doi.org/10.28919/cmbn/7056.

[16] T. Gard, T. Hallam, Persistence in food webs—I Lotka-Volterra food chains, Bull. Math. Biol. 41 (1979), 877-891. https://doi.org/10.1016/s0092-8240(79)80024-5.

[17] H.I. Freedman, P. Waltman, Persistence in models of three interacting predator-prey populations, Math. Biosci. 68 (1984), 213-231. https://doi.org/10.1016/0025-5564(84)90032-4.

[18] B. Dubey, R.K. Upadhyay, Persistence and extinction of one-prey and two-predators system, Nonlinear Anal.: Model. Control. 9 (2004), 307-329. https://doi.org/10.15388/na.2004.9.4.15147.

[19] J. Alebraheem, Y. Abu-Hasan, Persistence of predators in a two predators-one prey model with non-periodic solution, Appl. Math. Sci. 6 (2012), 943-956.

[20] S.B. Hsu, S. Ruan, T.H. Yang, Analysis of three species Lotka–Volterra food web models with omnivory, J. Math. Anal. Appl. 426 (2015), 659-687. https://doi.org/10.1016/j.jmaa.2015.01.035.

[21] A. Klebanoff, A. Hastings, Chaos in one-predator, two-prey models: cGeneral results from bifurcation theory, Math. Biosci. 122 (1994), 221-233. https://doi.org/10.1016/0025-5564(94)90059-0.

[22] K.S. Reddy, N.C.P. Ramacharyulu, A three-species ecosystem comprising of two predators competing for a prey, Adv. Appl. Sci. Res. 2 (2011), 208-218.

[23] B.M. Popkin, The dynamics of the dietary transition in the developing world, in: The Nutrition Transition, Elsevier, 2002: pp. 111-128. https://doi.org/10.1016/B978-012153654-1/50008-8.

[24] F.H. Maghool, R.K. Naji, The dynamics of a tritrophic Leslie-Gower food-web system with the effect of fear, J. Appl. Math. 2021 (2021), 2112814. https://doi.org/10.1155/2021/2112814.

[25] E.A.A.H. Jabr, D.K. Bahlool, The dynamics of a food web system: Role of a prey refuge depending on both species, Iraqi J. Sci. 62 (2021), 639-657. https://doi.org/10.24996/ijs.2021.62.2.29.

[26] C. Jost, S.P. Ellner, Testing for predator dependence in predator-prey dynamics: a non-parametric approach, Proc. R. Soc. Lond. B 267 (2000), 1611-1620. https://doi.org/10.1098/rspb.2000.1186.

[27] X. Wang, L. Zanette, X. Zou, Modelling the fear effect in predator-prey interactions, J. Math. Biol. 73 (2016), 1179-1204. https://doi.org/10.1007/s00285-016-0989-1.

[28] E. González-Olivares, B. González-Yañez, R. Becerra-Klix, et al. Multiple stable states in a model based on predator-induced defenses, Ecol. Complex. 32 (2017), 111-120. https://doi.org/10.1016/j.ecocom.2017.10.004.

[29] S.M.A. Al-Momen, R.K. Naji, The dynamics of modified Leslie-Gower predator-prey model under the influence of nonlinear harvesting and fear effect, Iraqi J. Sci. 63 (2022), 259-282. https://doi.org/10.24996/ijs.2022.63.1.27.

[30] X. Wang, X. Zou, Modeling the fear effect in predator-prey interactions with adaptive avoidance of predators, Bull. Math. Biol. 79 (2017), 1325-1359. https://doi.org/10.1007/s11538-017-0287-0.

[31] S.K. Sasmal, Population dynamics with multiple Allee effects induced by fear factors – A mathematical study on prey-predator interactions, Appl. Math. Model. 64 (2018), 1-14. https://doi.org/10.1016/j.apm.2018.07.021.

[32] S. Pal, S. Majhi, S. Mandal, N. Pal, Role of Fear in a Predator–Prey Model with Beddington–DeAngelis Functional Response, Z. Naturforsch. A 74 (2019), 581-595. https://doi.org/10.1515/zna-2018-0449.

[33] S. Vinoth, R. Sivasamy, K. Sathiyanathan, et al. The dynamics of a Leslie type predator–prey model with fear and Allee effect, Adv. Differ. Equ. 2021 (2021), 338. https://doi.org/10.1186/s13662-021-03490-x.

[34] N. Santra, S. Mondal, G. Samanta, Complex dynamics of a predator–prey interaction with fear effect in deterministic and fluctuating environments, Mathematics 10 (2022), 3795. https://doi.org/10.3390/math10203795.

[35] A.R.M. Jamil, R.K. Naji, Modeling and analyzing the influence of fear on the harvested modified Leslie-Gower model, Baghdad Sci. J. 20 (2023), 1701-1712. https://doi.org/10.21123/bsj.2023.7432.

[36] X. Wang, Y. Tan, Y. Cai, W. Wang, Impact of the fear effect on the stability and bifurcation of a Leslie–Gower predator–prey model, Int. J. Bifurcation Chaos 30 (2020), 2050210. https://doi.org/10.1142/s0218127420502107.

[37] K. Sarkar, S. Khajanchi, Impact of fear effect on the growth of prey in a predator-prey interaction model, Ecol. Complex. 42 (2020), 100826. https://doi.org/10.1016/j.ecocom.2020.100826.

[38] M.A. Ahmed, D.K. Bahlool, The influence of fear on the dynamics of a prey-predator scavenger model with quadratic harvesting, Commun. Math. Biol. Neurosci. 2022 (2022), 62. https://doi.org/10.28919/cmbn/7506.

[39] P. Cong, M. Fan, X. Zou, Dynamics of a three-species food chain model with fear effect, Commun. Nonlinear Sci. Numer. Simul. 99 (2021), 105809. https://doi.org/10.1016/j.cnsns.2021.105809.

[40] A. Sha, S. Samanta, M. Martcheva, et al. Backward bifurcation, oscillations and chaos in an eco-epidemiological model with fear effect, J. Biol. Dyn. 13 (2019), 301-327. https://doi.org/10.1080/17513758.2019.1593525.

[41] S.K. Sasmal, Y. Takeuchi, Dynamics of a predator-prey system with fear and group defense, J. Math. Anal. Appl. 481 (2020), 123471. https://doi.org/10.1016/j.jmaa.2019.123471.

[42] A.R.M. Jamil, R.K. Naji, Modeling and analysis of the influence of fear on the harvested modified Leslie–Gower model involving nonlinear prey refuge, Mathematics 10 (2022), 2857. https://doi.org/10.3390/math10162857.

[43] H.A. Ibrahim, D.K. Bahlool, H.A. Satar, et al. Stability and bifurcation of a prey-predator system incorporating fear and refuge, Commun. Math. Biol. Neurosci. 2022 (2022), 32. https://doi.org/10.28919/cmbn/7260.

[44] S. Mondal, G.P. Samanta, Dynamics of an additional food provided predator–prey system with prey refuge dependent on both species and constant harvest in predator, Physica A: Stat. Mech. Appl. 534 (2019), 122301. https://doi.org/10.1016/j.physa.2019.122301.

[45] M.M. Haque, S. Sarwardi, Dynamics of a harvested prey–predator model with prey refuge dependent on both species, Int. J. Bifurcation Chaos 28 (2018), 1830040. https://doi.org/10.1142/s0218127418300409.

[46] Z.M. Hadi, D.K. Bahlool, The effect of alternative resource and refuge on the dynamical behavior of food chain model, Malays. J. Math. Sci. 17 (2023), 731-754. https://doi.org/10.47836/mjms.17.4.13.

[47] H. Abdul Satar, R.K. Naji, Stability and bifurcation of a prey-predator-scavenger model in the existence of toxicant and harvesting, Int. J. Math. Math. Sci. 2019 (2019), 1573516. https://doi.org/10.1155/2019/1573516.

[48] H.A. Satar, R.K. Naji, Stability and bifurcation in a prey–predator–scavenger system with Michaelis–Menten type of harvesting function, Differ. Equ. Dyn. Syst. 30 (2019), 933-956. https://doi.org/10.1007/s12591-018-00449-5.